Technische Universität München

Klinik und Poliklinik für Chirurgie, Klinikum rechts der Isar

Brg1 modulates liver regeneration and promotes liver fibrosis

Baocai Wang

Vollständiger Abdruck der von der Fakultät für Medizin der Technischen Universität München zur Erlangung des akademischen Grades eines Doktors der Medizin genehmigten Dissertation.

Vorsitzender: Prof. Dr. Jürgen Schlegel

Prüfer der Dissertation:

1. apl. Prof. Dr. Norbert Hans Hüser

2. Priv.-Doz. Dr. Carolin Mogler

Die Dissertation wurde am 17.10.2019 bei der Technischen Universität München eingereicht und durch die Fakultät für Medizin am 11.02.2020 angenommen.

TABLE OF CONTENTS

FIGURE LEGENDS

TABLE LEGENDS

ABBREVIATIONS

a-SMA	Alpha smooth muscle-actin
β-ME	2-Mercaptoethanol
Ace	Angiotensin-converting enzyme
ALT	Alanine aminotransferase
APS	Ammonium persulfate
ATP	Adenosine triphosphate
BAF	Brg1-associated factor
BRCA1	Breast cancer gene 1
BrdU	Bromdesoxyuridin
Brg1	Brahma-related gene 1
Brm	Brahma
BSA	Bovine serum albumin
C/EBP	CCAAT-enhancer-binding protein
CCl_4	Carbon tetrachloride
Cdk	Cyclin-dependent kinase
CHD	Chromodomain helicase DNA-binding
CT	Cycle threshold
CVECs	Central vein endothelial cells

CYP2E1	Cytochrome P450 2E1
DNA	Deoxyribonucleic acid
ECM	Extracellular matrix
EDTA	Ethylenediaminetetraacetic acid
EMCN	Endomucin
FoxM1	Forkhead box M1
gDNA	Genomic DNA
GS	Glutamine synthetase
GSEA	Gene Set Enrichment Analysis
GSVA	Gene Set Variation Analysis
H2O2	Hydrogen peroxide
HBV	Hepatitis B virus
HCC	Hepatocellular carcinoma
HCV	Hepatitis C virus
HDAC	Histone deacetylase
HE	Hematoxylin and eosin
HSCs	Hepatic stellate cells
IF	Immunofluorescence
IHC	Immunohistochemistry
INO	Inositol

LSECs	Liver sinusoidal endothelial cells
LYVE1	Lymphatic vessel endothelial hyaluronan receptor 1
MOPS	3-(N-morpholino) propanesulfonic acid
NaCl	Sodium Chloride
NAFLD	Non-alcoholic fatty liver disease
NCoR-1	Nuclear receptor co-repressor 1
NF-κB	Nuclear factor kappa-B
NUMAC	Nucleosome methylation-activated complex
NuRD	Nucleosome remodeling and deacetylase
PARP	Poly (ADP ribose) polymerase
PBAF	Polybromo Brg1-associated factor
PBS	Phosphate Buffered Saline
PCNA	Proliferating cell nuclear antigen
PCR	Polymerase chain reaction
PFA	Paraformaldehyde
PH	Partial hepatectomy
PH3	Phosphorylated histone 3
Rb	Retinoblastoma
Rhbg	Rh Family B Glycoprotein
RNA	Ribonucleic acid

RNA-seq	RNA-sequencing
ROS	Reactive oxygen species
SD	Standard deviation
SDS-PAGE	Sodium dodecyl sulfate polyacrylamide gel electrophoresis
STAT3	Signal transducer and activator of transcription 3
STE	Sodium Chloride-Tris-EDTA
SWI/SNF	Switching/sucrose nonfermenting
SWR	Sick with Rat8 ts
TBST	Tris-buffered saline with 0.1% Tween 20
TGF	Transforming growth factor
TNF	Tumour necrosis factor
TSO	Template switch oligo
UMIs	Unique molecular identifiers
WB	Western Blot
WINAC	WSTF including nucleosome assembly complexes
WSTF	Williams Syndrome Transcription Factor

1 INTRODUCTION

1.1 Liver function and architecture

1.1.1 Structure and function of the liver

The liver is the largest visceral organ in humans. A normal healthy liver weighs approximately 1.5kg and is traditionally divided into four anatomic lobes: the right lobe, left lobe, caudate lobe and quadrate lobe (Skandalakis, Skandalakis et al. 2004). According to vascular supply and biliary drainage the liver is divided into 8 functional segments originally described by Couinaud (Couinaud 1954). Unlike most other organs, two afferent vessels supply hepatic blood: the hepatic artery (25% of blood supply) and the portal vein (75% of blood supply). Blood draining into the liver from the portal vein and hepatic artery moves towards the central veins, undergoing ultrafiltration and reabsorption. The central veins develop into large vessels, ultimately draining into the three large hepatic veins (right, middle and left hepatic veins) and finally into the inferior vena cava (Eipel, Abshagen et al. 2010).

The liver consists of different cell types. The main function of the liver is performed by hepatocytes, which account for about 60% of the total number of hepatic cells and 80% of the total liver volume (Kmiec 2001). The tight junction formed between the hepatocytes produces a small tube surrounded by the apical membrane of the adjacent hepatocytes. The hepatocytes produce the primary bile. Primary bile is modified in the bile ducts where the cholangiocytes add water, chloride, and bicarbonate to bile. The bile passes through the intrahepatic bile duct, the extrahepatic bile duct, and finally enters the duodenum (Boyer 2013).

Hepatocytes are polarised cells arranged in one cell layer-thick plates (Müsch 2014). Their basolateral surface faces the hepatic sinusoid. The hepatic sinusoid is a complex form of capillary in the liver with blood moving through at low pressure (Schaffner and Poper 1963) (Figure 1). The hepatic sinusoid consists of liver sinusoidal endothelial cells (LSECs), Kupffer cells, pit cells, and hepatic stellate cells (HSC). HSC are specialised connective tissue cells located in the perisinusoidal space (also called the space of Disse) between the hepatocytes and the endothelial cells. They contain vitamin A-rich lipid droplets, regulate blood flow and play a major role in fibrogenesis (Mogler, Wieland et al. 2015). The endothelial cells are fenestrated and constitute the barrier between the hepatocytes and the blood stream, allowing the exchange of fluids between the blood and the space of Disse, but hindering the passage of cells (Braet and Wisse 2002). Kupffer cells (macrophages) and pit cells (natural killer cells) have important roles in immune response and phagocytosis (Fahrner, Dondorf et al. 2016).

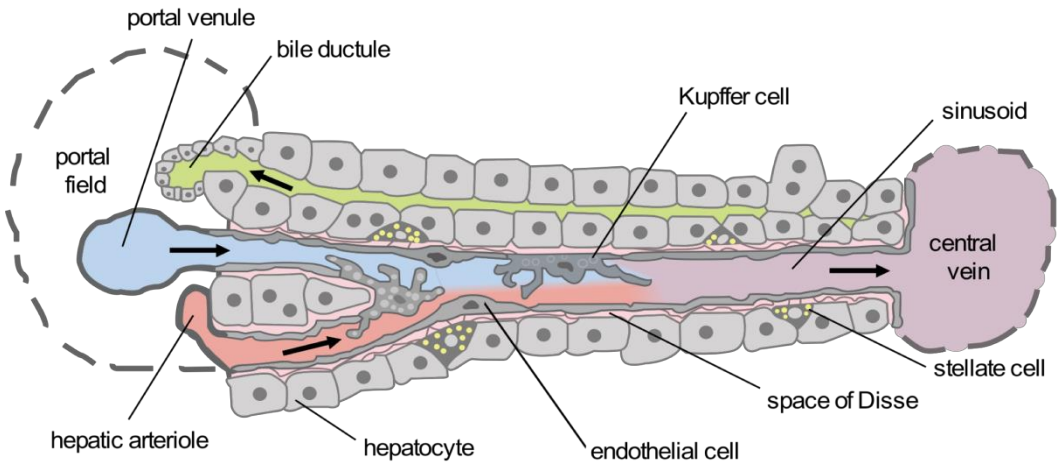

Figure 1. The structure of the hepatic sinusoid
The hepatic sinusoid is a type of a sinusoid capillary. Blood moves from the portal tract towards the centre, passing through the hepatic sinusoid (Frevert, Engelmann et al. 2005).

The liver is an organ found only in vertebrates and has a wide range of functions. Detoxification of endogenous and exogenous substances is one of the important roles of the liver. (Bogdanos, Gao et al. 2013). The liver is also a key organ of metabolic processes, including the storage of carbohydrates for glycogen, glucose (gluconeogenesis), fat metabolism and cholesterol synthesis, as well as protein synthesis such as albumin and beta-globulin (Mitra and Metcalf 2009). In addition, the liver is the cornerstone of the coagulation system by synthesising coagulation factors (Kaul and Munoz 2000).

1.1.2 Liver diseases

In acute and transient liver damage caused by insults, such as chemical hepatotoxins, the liver returns to the original structure by proliferating and remodeling of the remaining cells within one week. In contrast, chronic liver inflammation caused by various reasons, such as viral infections, and metabolic and immune disorders, leads to liver fibrosis, often progressing to cirrhosis and cancer (Tanaka and Miyajima 2016).

Liver disease has become one of the major causes of morbidity and mortality (Wong and Huang 2018). Since the 1970s, mortality due to liver disease has grown exponentially, especially in the group of people under 65 years of age. There are different reasons for the increased morbidity and mortality, including the dissemination of viral hepatitis (B and C), alcohol consumption, fatty liver disease and an increase of liver cancer. Liver transplantation is currently the most effective treatment for life-threatening liver failure resulting from chronic liver disease (Gambarin-Gelwan 2013). However, the demand for donor organs exceeds the number of available liver donations. Therefore, many patients die while waiting for a liver transplant. Liver resection surgery is the main curative treatment for liver cancer and other tumours. However, liver resection often is limited due to insufficient remaining liver tissue (Nadalin,

Bockhorn et al. 2006). It is important to develop a therapy that enhances the regeneration of damaged liver and prevents liver fibrosis.

1.2 Liver regeneration

1.2.1 Definition of liver regeneration

The liver has a unique regenerative capacity to regain its size, architecture, and function in response to the loss of mass caused by a variety of injuries (Fausto 2004). This regenerative capacity provides the basis for a potentially satisfying clinical outcome for patients after serious hepatic injury, cancer resection, or living donor liver transplantation. The regenerative capacity is often reduced when concomitant liver disease, such as liver fibrosis or non-alcoholic fatty liver disease (NAFLD), is present. Many studies have been performed to analyse the mechanism of liver regeneration. To promote liver regeneration therapeutically, it is important to decipher the molecular mediators that regulate liver regeneration.

1.2.2 Rodent models of liver regeneration

Historically, the ability of the liver to regenerate is well known, and the mechanism of liver regeneration has been studied for many years. A broad range of experimental animal models of various species are available to the research worker for liver regeneration, mainly divided into 3 main different types: surgical models, pharmacological models and pre-existing liver injury models (Palmes and Spiegel 2004). In 1931, Higgins and Anderson developed an experimental model of liver regeneration (Higgins 1931), following surgical removal of the median and left lobes of the rat, equivalent to two-thirds of the total liver mass (Figure 2). Since then, two-thirds partial hepatectomy (PHx) has been used as a standard model for liver regeneration. In this model, the remnant liver lobes enlarge to compensate for the lost mass, which is called

compensatory hyperplasia. After decades of research on the liver regeneration from two-thirds PHx, it is believed that one or two replications of the remaining hepatocytes should be empirically sufficient to restore the original quality and function (Kholodenko and Yarygin 2017). The use of this model resulted in a better understanding of liver regeneration.

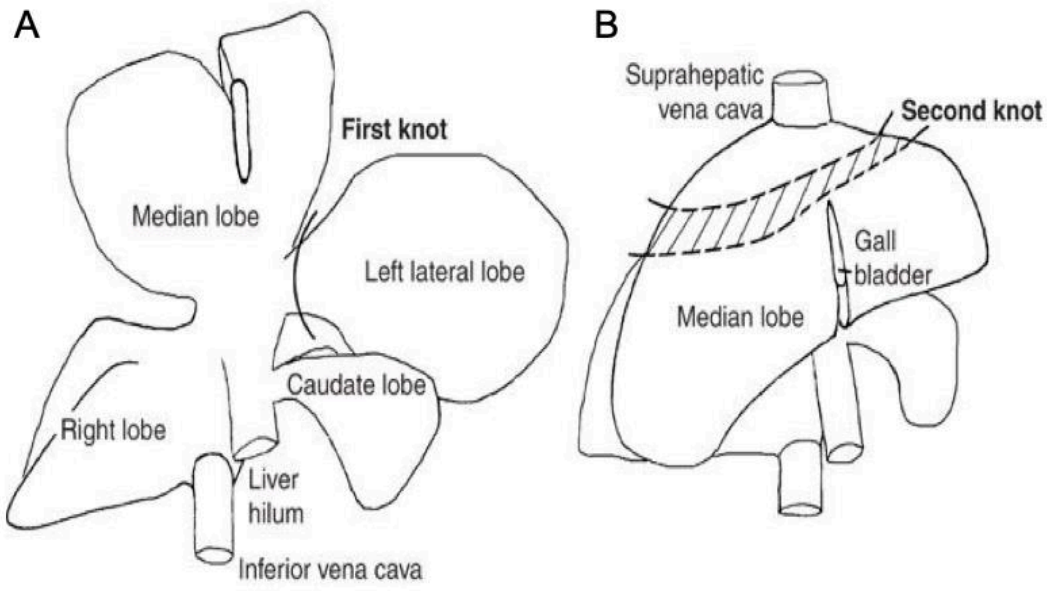

Figure 2. Partial hepatectomy
Schematic representation of mouse liver anatomy. (A) The first knot should be between the caudate and left lobe at the bottom of the latter. (B) The second knot should be tied in the area of the dotted line above the gallbladder (Mitchell and Willenbring 2008).

1.2.3 Mechanisms of liver regeneration

Liver regeneration starts with a well-organised and complex series of signals, following three sequential and critical steps (Pahlavan, Feldmann Jr et al. 2006). Firstly upon PHx, hepatocytes exit their quiescent and highly differentiated state in order to rapidly re-enter the cell cycle (priming phase). Secondly, with the help of mitogens, hepatocytes enter the cell cycle and progress beyond the restriction point to G1 phase and M-phase in order to proliferate and compensate for the removed mass (proliferation phase) (Taub

2004). After approximately two cell cycles of hepatocyte replication, cells terminate proliferation under the control of negative factors (termination phase) (Hu, Srivastava et al. 2014). Finally, liver mass is restored to the size before hepatectomy, and liver morphology is gradually rearranged (Sun and Irvine 2014).

The evolution of the concept of the liver regeneration mechanism changed from the initial point that a single humoral agent could be capable of unlocking all of the events required for liver regeneration to the more recent idea that the activity of multiple interconnected pathways are required for liver regeneration (Cienfuegos, Rotellar et al. 2014). This idea can be demonstrated through the finding that genetic modifications causing defects in a single signaling pathway often result in delayed liver regeneration but do not completely block the regenerative process. Liver regeneration requires the activation of a complex network of pathways to proceed in an optimal manner. Recent literature suggests that the essential circuitry required for liver regeneration consists of three types of pathways, including various cytokines, responsible for hepatocyte priming; growth factors, responsible for cell cycle progression; and hormones with their effects on energy metabolism (Michalopoulos and DeFrances 1997, Sakamoto, Liu et al. 1999, Fausto, Campbell et al. 2006, Malato, Sander et al. 2008). In recent years, a major role has been shown for epigenetic mechanisms that are involved in liver regeneration. Hereby, a key role of the Brahma-related gene 1 (Brg1), a catalytic subunit of the SWI/SNF chromatin remodelling complex, in different phases of liver regeneration was demonstrated(Sinha, Verma et al. 2016). However, to date, the mechanism of liver regeneration and the special role of the subunit Brg1 is still not fully understood.

1.3 Liver fibrosis

1.3.1 Definition of liver fibrosis

Hepatic fibrosis is a stage of liver remodeling caused by chronic liver disease of various aetiologies, including ethanol, viral infection, drugs and toxins, cholestasis, metabolic and genetic diseases (Mormone, George et al. 2011). In principle liver fibrosis is a reversible wound healing process associated with a number of pathological and biochemical changes leading to structural and metabolic abnormalities, as well as an increased risk of hepatic scarring (Bissell 1990, George and Chandrakasan 2000). Chronic liver injuries potentially cause progression from the stage of fibrosis to irreversible cirrhosis - a condition that is characterised by distortion of the normal architecture, nodule formation, altered blood flow, portal hypertension, and high risk of hepatocellular carcinoma and ultimately liver failure (Han, Zhou et al. 2004).

1.3.2 Mouse models of liver fibrosis

There are many ways to induce liver fibrosis, such as chemical-based animal models, surgery-based models, diet-based models, methionine- and choline-deficient diets and transgenic models (Yanguas, Cogliati et al. 2016). The chemical-based animal models are very popular because of their high reproducibility, ease of use and appropriate reflection of the mechanisms involved in human liver fibrosis (Smith 2013). Chemical-based models included ethanol, carbon tetrachloride (CCl_4), thioacetamide, dimethylnitrosamine and diethylnitrosamine. In most cases, intraperitoneal injection of these chemicals triggers liver fibrosis on a relatively short-term basis (Smith 2013). When administered orally or via inhalation, fibrosis is limited and takes more time to develop (Smith 2013). CCl_4 is the most commonly used hepatotoxin in rodent liver fibrosis and cirrhosis studies. In

many ways, it mimics human chronic diseases associated with toxic damage (Yanguas, Cogliati et al. 2016). The liver biotransformation of CCl_4 is dependent on Cytochrome P450 2E1 (CYP2E1) and produces trichloromethyl, which is involved in several free radical reactions and lipid peroxidation processes (Basu 2003). These processes contribute to an acute phase reaction characterised by necrosis of centrilobular hepatocytes, the activation of Kupffer cells and the induction of an inflammatory response (Heindryckx, Colle et al. 2009). This sequence is associated with the production of several cytokines, which promote the activation of HSCs and hence liver fibrosis (Iwaisako, Jiang et al. 2014). Recently, a C57BL/6 mouse model was standardised relying on intraperitoneal administration of CCl_4 (Yanguas, Cogliati et al. 2016).

1.3.3 Mechanisms of liver fibrosis

The development of liver fibrosis and subsequent cirrhosis is driven by a variety of mechanisms of persistent liver injury and can be thought of as an excessive wound healing response caused by hepatocyte necrosis, inflammation and pathogenic malignant circulation of excessive extracellular matrix（ECM) deposition (Zhang, Yuan et al. 2016). Hepatocytes are targets for most hepatotoxic diseases and substances, including hepatitis viruses, alcohol metabolites and bile acids (Zhou, Zhang et al. 2014).

Prolonged exposure to toxic substances can cause liver cell damage and apoptosis. Damaged hepatocytes release reactive oxygen species (ROS) and fibrotic mediators like nuclear factor kappa-B (NF-kB), tumour necrosis factor-a (TNF-a), and transforming growth factor-β1 (TGF-β1), which recruit inflammatory cells and leukocytes (de Andrade, Moura et al. 2015). NF-κB enhances liver fibrosis by promoting the survival of HSCs (Pradere, Kluwe et al. 2013), TNF-a has a regulatory role in extracellular matrix remodeling and liver fibrosis (Tarrats, Moles et al. 2011), while TGF-β1, which activates HSC, is the

most potent known fibrogenic agonist (Hellerbrand, Stefanovic et al. 1999). HSCs play a key role in the development of fibrous tissue by synthesising the extracellular matrix (known as the process of fibrogenesis) (Mogler, Wieland et al. 2015). In addition, activated HSCs secrete inflammatory chemokines, express cell adhesion molecules and regulate lymphocyte activation (Fujita and Narumiya 2016). As a result, a vicious circle occurs and mutual stimulation between inflammation and profibrotic cells drives liver fibrosis (Koyama and Brenner 2017). In recent studies epigenetic mechanisms that modulate different aspects of liver fibrogenesis have been shown (Moran-Salvador and Mann 2017). Hereby, Brg1 plays a key role as a critical modulator of transcriptional regulation in cellular processes (Li, Lan et al. 2018). However, the exact role of Brg1 remains unclear.

1.4 Chromatin remodelling and liver disease

1.4.1 Definition of chromatin remodelling

Epigenetic regulation plays a key role in maintaining correct gene expression and is achieved through several mechanisms, including deoxyribonucleic acid (DNA) methylation, histone modifications, and adenosine triphosphate (ATP)-dependent chromatin remodelling. Chromatin remodelling enzymes use the energy from ATP hydrolysis to alter the interaction between DNA and histone proteins (Becker and Workman 2013). This change in chromatin structure results in the alteration of transcriptional accessibility and advanced chromatin structure. In addition, chromatin remodelling of nucleosome movement is essential for several important biological processes, including chromosome assembly and isolation, DNA replication and repair, embryonic development and pluripotency, and cell cycle progression (Budhavarapu, Chavez et al. 2013). The deregulation of chromatin remodeling results in a loss of transcriptional regulation at critical checkpoints required for proper cellular

function, therefore causing various disease syndromes, including cancer (Tyagi, Imam et al. 2016).

1.4.2 SWI/SNF Complex

Chromatin remodelling regulates gene expression by disrupting the stability of the nucleosome structure, thereby altering the accessibility of DNA to transcription factors in an ATP-dependent manner (Clapier and Cairns 2009). The family of chromatin remodelling complexes that rely on ATP can be subdivided into five distinct categories: switching/sucrose nonfermenting (SWI/SNF), imitation switch(ISWI), nucleosome remodelling histone deacetylase/ chromo-helicase/ chromodomain helicase DNA-binding (NuRD/Mi2/CHD), inositol requiring protein 80 (INO80) and Sick with Rat8 ts (SWR1) (Clapier and Cairns 2009). Each individual complex is characterised by its specific catalytic subunit (Trotter and Archer 2008). The SWI / SNF complex is a chromatin remodeller that uses the energy obtained by ATP hydrolysis to alter the structure of the chromatin. The bromodomain and an AT-hook region are unique domains of the SWI/SNF complex (Tang, Nogales et al. 2010). Bromodomains interact with acetylated lysines whereas the AT-hook region binds to AT-rich regions of DNA. These domains enable the SWI/SNF complex to target histones and DNA and regulate transcription (Euskirchen, Auerbach et al. 2012). By doing so the SWI/SNF complex functions as a modulator of transcription factors, thereby regulating gene expression (Peterson and Tamkun 1995).

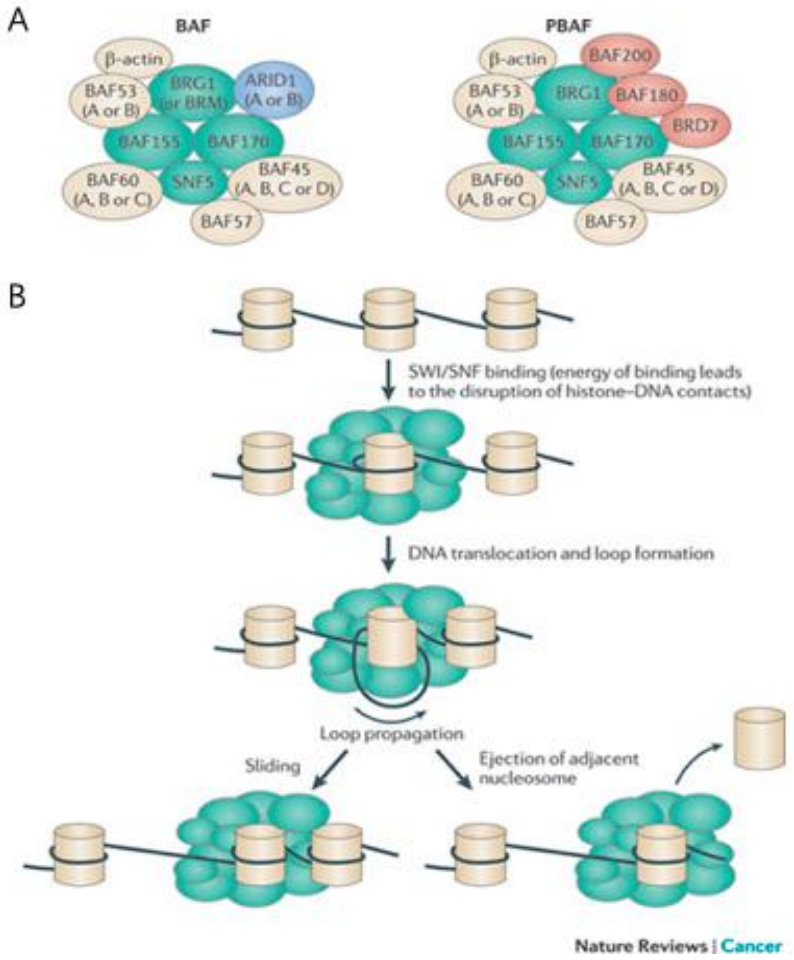

Figure 3. SWI/SNF Complex
(A) The diversity of composition of SWI/SNF complexes. The BRG1-associated factor (BAF; also known as SWI/SNF-A) and polybromo BRG1-associated factor (PBAF; also known as SWI/SNF-B) complexes constitute major subclasses. **(B)** Mechanisms of remodelling are shown. The steps of remodelling include SWI/SNF binding, disruption of histone–DNA contacts, the creation of a loop of DNA that propagates around the nucleosome in a wave-like manner and the repositioning of DNA with respect to the nucleosome (sliding). (Wilson and Roberts 2011)

SWI/SNF complexes can be detected in different species during evolution. The genes for mating type transformation (SWI) and nutrient transformation (sucrose non-fermentation; SNF) were first detected in yeast and identified as transcriptionally activated subunits (Workman and Kingston 1998). These genes gave the complex its name (Neigeborn and Carlson 1984, Stern, Jensen et al. 1984, Peterson and Herskowitz 1992). The evolutionary homologues of the yeast SWI/SNF complex are then identified in Drosophila

(BAP complex) and finally identified in mammals (BAF complexes). The mammalian SWI/SNF complex family is further subdivided into two major complexes, the brahma-related gene 1 (Brg1)-associated factor complex (BAF) and the polybromo Brg1-associated factor (PBAF) complex (Mohrmann, Langenberg et al. 2004). While the catalytic subunit Brahma (Brm) is used only in BAF complexes, Brahma-related gene 1 (Brg1) is a subunit of both mammalian SWI/SNF complexes (Figure 3) (Kadoch and Crabtree 2015).

The macromolecular SWI/SNF complex consists of 12 to 15 subunits that are composed by the combination of 29 gene products (Pulice and Kadoch 2016). Due to the combination of different subunits, there are various numbers of BAF complexes. These different BAF complexes have different functions. BAF complex is present throughout the body's nucleus and is involved in the regulation of gene transcription at many stages and developments, including vertebrate nervous system development, cardiac development and induced pluripotency, as well as several other developmental backgrounds (Ho and Crabtree 2010, Singhal, Graumann et al. 2010, Han, Hang et al. 2011, Hu, Strobl-Mazzulla et al. 2014, Trost, Haines et al. 2018).

Genes that are regulated by the SWI/SNF-complex are involved in a variety of cellular pathways, including signal transduction, cell cycle, apoptosis, cell adhesion, cell morphology, DNA repair, and stress response (Gong, Fahy et al. 2006, Park, Park et al. 2006, Euskirchen, Auerbach et al. 2011). These findings underline the biological importance of the human SWI/SNF complex. For a protein complex with such a functional significance and wide array of effects, it is not unusual to find that its abnormalities are linked to serious consequences.

1.4.3 The chromatin regulator Brg1

The mammalian SWI/SNF complex consists of the two main catalytic subunits Brm (Brahma) and Brg1. Brg1 (syn: SMARCA4 = SWI/SNF-related, matrix-associated, actin-dependent chromatin regulatory factor, subfamily A, member 4) is located on chromosome 19p13.2 and was first identified in 1984 in yeast screens. Although the two proteins Brg1 and Brm have 74% sequence identity, they have different regulatory effects on different cellular processes (Trotter and Archer 2008).

Brg1 is an ATPase that hydrolyses ATP and enables the SWI/SNF complex to modulate chromatin structure (Tang, Nogales et al. 2010). Brg1 has a bromodomain that can bind to acetylated lysines on the histone tails (Josling, Selvarajah et al. 2012). The Brg1 protein consists of 1614 amino acids with a molecular weight of 180 kD (Medina and Sanchez-Cespedes 2008) to 205 kDa (Khavari, Peterson et al. 1993). Brg1 is evolutionarily homologous to SWI2, a catalytic subunit of the SWI/SNF complex in *Saccharomyces cerevisiae* (Khavari, Peterson et al. 1993, Phelan, Sif et al. 1999, Muchardt and Yaniv 2001).

Brg1 is not only a known subunit of the SWI/SNF complex, but also a part of several other complexes. Notable examples include WINAC complexes (Williams Syndrome Transcription Factor (WSTF), including nucleosome assembly complexes), NUMAC complexes (nucleosome methylation-activated complexes), NCoR-1 complexes (Nuclear receptor co-repressor 1) and mSin3A/HDAC complexes (histone deacetylases-3) (Trotter and Archer 2008). All of these Brg1-related complexes have a nuclear mode of action and regulate DNA replication, DNA repair, elongation and transcription in different ways. The NUMAC complex and the NCoR-1 complex for example modify histone methylation and acetylation in order to regulate DNA processes (Trotter and Archer 2008, Smith-Roe, Nakamura et al. 2015).

1.4.4 The biological role of Brg1

The main catalytic ATPase subunit of the SWI/SNF complex Brg1 is essential for embryogenesis and organogenesis as well as gene expression and the development of different tissues (Bultman, Gebuhr et al. 2005, Bultman, Gebuhr et al. 2006, Eroglu, Wang et al. 2006, Inayoshi, Miyake et al. 2006, Hang, Yang et al. 2010, Zhang, Chen et al. 2011, Li, Xiong et al. 2013). An important function for Brg1 was detected in the development of the heart (Stankunas, Hang et al. 2008, Akerberg, Sarangam et al. 2015). It is further known that Brg1 influences neuronal development (Bultman, Gebuhr et al. 2000) and plays an important role in erythropoiesis (Bultman, Gebuhr et al. 2005) (Griffin, Brennan et al. 2008). In addition, for the development of a sufficient immune system Brg1 is a central element. An important function of Brg1 was also demonstrated in thymic and T-cell development (Chi, Wan et al. 2003). In mammals, the deletion of Brg1 in neural progenitors led to defective neural stem cell self-renewal and maintenance and impaired differentiation (Petrik, Latchney et al. 2015). Furthermore, The SWI/SNF chromatin remodelling complex has been described as a key regulator of skeletal muscle differentiation, whereby the ATPase of Brg1 is required for gene expression at different stages of skeletal myogenesis (Ohkawa, Yoshimura et al. 2007).

In numerous malignant tumours, Brg1 is mutated and overexpressed (Savas and Skardasi 2018). Brg1 has also been reported to interact with other tumour suppressors including pRb (Retinoblastoma), breast cancer gene 1(BRCA1), c-Myc, c-Fos and member proteins of the Wnt signalling pathway (Murphy, Hardy et al. 1999, Bochar, Wang et al. 2000, Barker, Hurlstone et al. 2001, Pal, Yun et al. 2003, Eroglu, Wang et al. 2006). A previous study by our group demonstrated that Brg1 is overexpressed in hepatocellular carcinoma (HCC) and positively promotes proliferation. In doing so, Brg1 regulates different cell cycle genes, mainly those of the cyclin family (Kaufmann, Wang et al. 2017).

1.4.5 Role of Brg1 in liver regeneration

Recently, an important role for the SWI/SNF complex was shown for liver regeneration. It was revealed that the subunit Arid1a plays a key role in the context of liver regeneration by impairing liver regeneration, mainly due to the positive modulation of target gene transcription that repress proliferation (Sun, Chuang et al. 2016). However, the exact function of the SWI/SNF complex and, in particular, its catalytic ATPase subunits in liver regeneration remains unclear.

Besides its role as an epigenetic regulator Brg1 is also known to directly bind to the promoter of different target genes to activate/silence gene expression. Hereby, Brg1 functions as a transcription factor itself for various genes (Raab, Runge et al. 2017) . The exact role of Brg1 in the context of the regulation of gene expression has not been completely clarified. Regeneration studies of other organs revealed that the repression of cyclin-dependent kinase (Cdk) inhibitors by Brg1 is the driving force for regeneration (Xiong, Li et al. 2013, Xiao, Gao et al. 2016). An inverse correlation was detected between Cdkn1B/p27 and Brg1. This inhibitory effect of Brg1 on the cyclin dependent kinase inhibitor 1B is correlated with the effect on the cyclin family in a proliferation-promoting intervention in the cell cycle (Xiong, Li et al. 2013, Xiao, Gao et al. 2016). Another growth-promoting effect of Brg1 was found by the positive correlation of Brg1 with members of the cyclin family. This has been demonstrated experimentally for Cyclin B1, Cyclin E1 and Cyclin D1 (Lin, Wong et al. 2010, Watanabe, Semba et al. 2011, Bai, Mei et al. 2012, Bai, Mei et al. 2013). In particular, CyclinD1 seems to play a crucial role during the G1 phase and thus for the proliferation of the cells (Bai, Mei et al. 2012). An interaction of Cyclin E and Brg1 has also been demonstrated without mediation by the pRB family (Shanahan, Seghezzi et al. 1999). Furthermore, the interaction between Brg1 and Brm in different phases of liver injury and regeneration contributes

essentially to liver regeneration(Sinha, Verma et al. 2016). Whereas Brm dominates during the late injury phase and the initiation of regeneration phase, Brg1 is the main catalytic subunit of the SWI/SNF complex during the injury and regeneration phase (Sinha, Verma et al. 2016). However, the precise role of Brg1 on proliferation during liver regeneration after liver injury as well as the signaling pathway remains unclear.

1.4.6 Role of Brg1 in liver fibrogenesis

Brg1, as the core ATPase of the SWI/SNF family, has been recently reported to be involved in the fibrosis of different organ systems (Zager and Johnson 2009, Hang, Yang et al. 2010, Qi, Wang et al. 2015, Weng, Yu et al. 2015, Yang, Feng et al. 2016). In hearts, following pathological stress, Brg1 and forkhead box M1 (FoxM1) transcription factor complexes regulate the transcription of angiotensin-converting enzyme (Ace) and Ace2 by binding to their promoter regions in the coronary endothelial cells. These, in turn, trigger angiotensin I-to-II conversion, followed by cardiac hypertrophy and fibrosis (Yang, Feng et al. 2016). Furthermore, Brg1 is also activated by cardiac stresses and forms a complex with histone deacetylase (HDAC) and poly(ADP ribose) polymerase (PARP) to induce a pathological a-myosin heavy chain to b-myosin heavy chain shift in cardiomyocytes, and promote myocyte proliferation and accelerate cardiac fibrosis (Hang, Yang et al. 2010). Besides myocardial fibrosis, Brg1 has been shown to be abnormally elevated in renal fibrosis following ischemia-reperfusion injury by binding to the promoters of pro-inflammatory or profibrotic genes to accentuate their transcription (Zager and Johnson 2009).

In the liver it was shown that hepatocytes cultured with free fatty acids overexpress Brg1 and Brm, stabilising NF-κB, and that this is required for the development of steatosis, inflammation and fibrosis in methionine-choline deficient diet-fed mice. Lentivirus-mediated knockdown of Brg1 attenuates

steatosis in mice by down-regulating the hepatic output of pro-inflammatory mediators (Tian, Xu et al. 2013). TGF-β has multiple pro-fibrogenic but also anti-inflammatory and immunosuppressive effects. It is observed that most TGF-β gene responses in human epithelial cells are dependent on Brg1 function (Xi, He et al. 2008). However, to date, the role of Brg1 in liver fibrosis remains unclear.

2 AIMS OF THE STUDY

Brg1, the core subunit of the SWI/SNF chromatin remodelling complex, is known to play a key role after liver injury (Sinha, Verma et al. 2016) and during non-alcoholic steatohepatitis which may progress to fibrosis and cirrhosis (Tian, Xu et al. 2013). However, the hepatocyte-specific contribution of Brg1 during liver regeneration and liver fibrosis is still not fully understood.

The aims of the present study are:

1. To determine whether Brg1 hepatocyte-specific knockout impacts on liver development in a mouse model.
2. Consider whether Brg1 hepatocyte-specific knockout impacts liver regeneration and which molecular signalling pathways are modulated by Brg1.
3. Assess whether a Brg1 hepatocyte-specific knockout protects from developing liver fibrosis *in vivo,* and then confirm what the hepatocyte-specific role of Brg1 is in the pathogenesis of liver fibrosis?

3 MATERIALS AND METHODS

3.1 Materials

3.1.1 Chemicals and Reagents

Table 1. Chemicals and reagents

Chemicals and Reagents	Supplier
EDTA	ROTH, Karlsruhe, Germany
2-Mercaptoethanol	Sigma-Aldrich, St Louis, USA
Acetic acid	ROTH, Karlsruhe, Germany
Aqua	Braun, Melsungen, Germany
Agarose	VWR, Radnor, USA
Acrylamide solution	ROTH, Karlsruhe, Germany
Ammonium persulfate (APS)	Sigma-Aldrich, St Louis, USA
Bovine serum albumin (BSA)	ROTH, Karlsruhe, Germany
Brdu	BD, Franklin lakes, USA
Calcium chloride	ROTH, Karlsruhe, Germany
Carbon tetrachloride	Sigma-Aldrich, St Louis, USA
Citric acid	ROTH, Karlsruhe, Germany
Corn oil	Sigma-Aldrich, St Louis, USA
DAB+ Chromogen	DAKO, Carpinteria, USA
ECL detection reagent	Amersham, Chicago, USA
Eosin	Merck, Darmstadt, Germany
Ethidium bromide	ROTH, Karlsruhe, Germany

Ethanol	ROTH, Karlsruhe, Germany
GeneRiler™ DNA Ladder	Thermo Scientific, Waltham, USA
Glycin	ROTH, Karlsruhe, Germany
Goat Serum	Abcam, Cambridge, UK
Haematoxylin	Merck, Darmstadt, Germany
Hydrochloric Acid	ROTH, Karlsruhe, Germany
Hydrogen peroxide(H2O2) (30%)	ROTH, Karlsruhe, Germany
Histowax	Leica, Nussloch, Germany
Isoflurane	Henry Schein, Munich, Germany
Isopropanol	ROTH, Karlsruhe, Germany
JumpStart™ REDTaq® ReadyMix™ Reaction Mix for PCR	Sigma-Aldrich, St Louis, USA
Liquid Nitrogen	Tec-Lab, Rosenheim, Germany
Methanol	ROTH, Karlsruhe, Germany
Microplate washer	Tecan, Männedorf, Switzerland
Milk Powder Blotting Grade	ROTH, Karlsruhe, Germany
Molecular Imager® Gel Doc™ XR+ System	Bio-rad, Hercules, USA
MOPS	Sigma-Aldrich, St Louis, USA
Mounting Medium	Vector, Burlingame, USA
NuPAGE LDS Sample Buffer	Invitrogen, Carlsbad, USA
NuPAGE Sample Reducing Agent	Invitrogen, Carlsbad, USA
Oxygen	Sauerstoffwerk Friedrichshafen, Friedrichshafen, USA
PageRuler™ PlusPrestained Protein Ladder	Thermo Scientific, Waltham, USA
Para-formaldehyde	Apotheke TU München, Munich, Germany

Phosphate Buffered Saline (PBS) pH7.4	Merck, Darmstadt, Germany
Phosphatase inhibitor cocktail tablet	Roche, Basel, Switzerland
Potassium Chloride	ROTH, Karlsruhe, Germany
Protease Inhibitor Cocktail Tablet	Roche, Basel, Switzerland
Proteinase K	Roche, Basel, Switzerland
RIPA Buffer	Cell Signaling Technology, Danvers, USA
RNAse DNAse-free Water	Ambion, Waltham, USA
Roticlear	ROTH, Karlsruhe, Germany
Rotiphorese gel 30	ROTH, Karlsruhe, Germany
SDS pellets	ROTH, Karlsruhe, Germany
Sodium Chloride(NaCl)	ROTH, Karlsruhe, Germany
Sodium Citrate	Sigma, Darmstadt, Germany
Sodium Hydroxide	ROTH, Karlsruhe, Germany
Sodium Phosphate	Sigma, Darmstadt, Germany
SuperSignal™ West Femto Maximum Sensitivity Substrate	Thermo Fisher, Waltham, USA
TEMED	ROTH, Karlsruhe, Germany
Tris Base	Sigma, Darmstadt, Germany
Triton 100x	ROTH, Karlsruhe, Germany
Tween 20	Sigma, Darmstadt, Germany

3.1.2 Kit system

Table 2. Kits

Kit	Supplier
BCA Protein Assay Kit	Thermo Scientific, Waltham, USA
ELISA Kit for Alanine Aminotransferase	Cloud Clone Corp, Wuhan, China
QuantiTect Reverse Transcription Kit	Qiagen, Hilden, Germany
RNeasy Plus Mini Kit	Qiagen, Hilden, Germany
SYBR Green Master Kit	KAPA, Wilmington, USA

3.1.3 Laboratory equipment

Table 3. Laboratory equipment

Name	Supplier
Agarose Gel Electrophoresis	Analytik Jena, Jena, Germany
Analytic balance	Sartorius, Göttingen, Germany
Balance	Sartorius, Göttingen, Germany
Centrifuge	Eppendorf, Berzdorf, Germany
CO_2 incubator	Heraeus, Hanau, Germany
Electrophresis/Electroblotting equipment / power supply	Bio-rad, Hercules, USA
Freezer -20 °C	SIEMENS, Munich, Germany
Freezer -80 °C	Thermo Scientific, Waltham, USA
Glomax multi dection system	Promega, Medison, USA
Lightcycler 480	Roche, Basel, Switzerland
Low Voltage Power Supplies	Analytik Jena, Jena, Germany

Microscope	Zeiss, Oberkochen, Germany
Microwave oven	Caso Ecostyle, Arnsberg, Germany
Nanodrop	Thermo Scientific, Waltham, USA
PH-meter	Inolab, Weilheim, Germany
Printer	Kyocera, Kyoto, Japan
Refrigerator 4 °C	LIEBHERR, Bulle FR, Switzerland
Roller mixer	STUART, Stone, UK
Scanner	HP, Palo Alto, USA
Table Top Research Anesthesia Machine w/O2 Flush	Volker, Lübeck, Germany
Thermocycler	VWR, Radnor, USA
Tissuelyser	Qiagen, Hilden, Germany
Vortex Mixer	NEOLAB, Heidelberg, Germany
Tissue embedding machine	Leica, Nussloch, Germany
Vacuum tissue processor ASP200s	Leica, Nussloch, Germany

3.1.4 Consumables

Table 4. Consumables

Name	**Supplier**
Cotton Bud	Lohmann Rauscher, Vienna, Austria
Coverslips	MENZEL, Munich, Germany
Filter (0.2µm)	NEOLAB, Heidelberg, Germany
Hyperfilm	GE Healthcare, Chicago, USA
HDR-C Plus Medical X-Ray Film	Agfa, Chicago, USA
Microscope Slide	Thermo Scientific, Waltham, USA

Nitrocellulose Blotting Membranes	Amersham, Little Chalfont, UK
Single use Syringes(1ml)	Braun, Melsungen, Germany
Sterile needles	BD, Franklin lakes, USA
Tissue Cassette	Medite, Burgdorf, Germany
Tissue culture dishes	Falcon, New York, USA
Falcon tubes (15ml, 50ml)	GREINER, Frickenhausen, Germany
Blotting paper	Whatman, Maidstone, UK

3.1.5 List of Antibodies

3.1.5.1 Primary antibodies

Table 5. Primary antibodies

Name	Catalog number	Application	Supplier
a-SMA	ab5694	WB IHC	Abcam, Cambridge, UK
β-actin	sc-69879	WB	Santa Cruz, Santa Cruz, USA
β-tubulin	ab6046	WB	Abcam, Cambridge, UK
Arginase I	sc-18351	IF	Santa Cruz, Santa Cruz, USA
Brdu	Bu20a	IHC	Cell Signaling Technology, Danvers, USA
Brg1	H-88	IHC WB	Santa Cruz, Santa Cruz, USA
Cdk1	ab131450	WB	Abcam, Cambridge, UK
Cyclin B1	4138	WB	Cell Signaling Technology, Danvers, USA

Endomucin	14-5851-82	IF	Thermo Fisher Scientific, Waltham, USA
GAPDH	sc-32233	WB	Santa Cruz, Santa Cruz, USA
Glutamine synthetase	G2781	IF	Sigma-Aldrich, St Louis, USA
Ki67	550609	ich	BD, Franklin lakes, USA
Lyve1	AF2125	IF	R&D Systems, Wiesbaden, Germany
NF-kB	8242	WB	Cell Signaling Technology, Danvers, USA
p53	NCL-p53-CM5p	WB	Leica, Nussloch, Germany
PCNA	2586	WB	Cell Signaling Technology, Danvers, USA
PH3	9701	WB	Cell Signaling Technology, Danvers, USA
RhBg	PA5-19369	IF	Thermo Fisher Scientific, Waltham, USA
STAT3	4904	WB	Cell Signaling Technology, Danvers, USA
TNF-a	3702	WB	Cell Signaling Technology, Danvers, USA

3.1.5.2 Secondary antibodies

Table 6. Secondary antibodies

Name	Catalog number	Application	Supplier
Alexa-Fluor 488		IF	Dianova, Hamburg, Germany

Alexa-Fluor 647		IF	Dianova, Hamburg, Germany
Anti-Mouse IgG HRP Conjugate	W402B	WB	Promega, Medison, USA
Anti-Rabbit IgG HRP Conjugate	W401B	WB	Promega, Medison, USA
Cy3-conjugated		IF	Dianova, Hamburg, Germany
Goat HRP- Labelled Anti-Mouse	K4001	IHC	DAKO, Carpinteria, USA
Goat HRP- Labelled Anti-Rabbit	K4011	IHC	DAKO, Carpinteria, USA

3.1.6 Primer sequences for real-time PCR

Table 7. Primer sequences

Gene(specie)	Sense (5' →3')	Antisense (5' →3')
Brg1(m)	CAAAGACAAGCATATCCTAGCCA	CACGTAGTGTGTGTTAAGGACC
CCl3(m)	CCTGCTGCTTCTCCTACA	TCCAAGACTCTCAGGCATT
Cxcl2(m)	CCCTGGTTCAGAAAATCATC	TCCAAGACTCTCAGGCATT
Cxcl5(m)	GAAGGAGGTCTGTCTGGAT	TCATCAAAGCAGGGAGTTC

3.2 Methods

3.2.1 Animal protocols

3.2.1.1 Mouse model

All mice were housed in specified pathogen-free facilities (ZPF, Klinikum rechts der Isar, Munich, Germany). Mice with a homozygous deficiency of

Brg1 were generated by the inter-cross of $Brg1^{fl/fl}$ and AlbCre single mutant mice on a mixed genetic background. Corresponding controls ($Brg1^{fl/fl}$, $Brg1^{fl/-}$) were provided. All experiments were performed in an age- and sex-controlled manner. Animal experiments were institutionally approved by the District Government of Upper Bavaria (AZ 55.2.1.54-2532-125-2015) and performed in accordance with the relevant guidelines and institutional regulations.

3.2.1.2 Partial hepatectomy

Male mice aged of 8 to 10 weeks were subjected to two-thirds partial hepatectomy using standard procedures according to the published protocol (Mitchell and Willenbring 2008). Ligation and resection of the middle and left lobes were performed under isoflurane inhalation anaesthesia. Partial hepatectomy was performed between 8 and 10 am. Mice underwent intraperitoneal injections of 100 µg/g BrdU 2 hours before sacrifice. At the indicated time points, mice were sacrificed.

3.2.1.3 CCl_4 injection

Male mice at the age of 8 to 10 weeks were administered CCl_4 through intraperitoneal (*i.p.*) injection of CCl_4 twice a week for 4, 6, 8 and 12 weeks. The concentration of CCl_4 is 0.5µl/g body weight and CCl_4 is diluted in corn oil (CCl_4:corn oil=1:7). Mice were sacrificed 3 days after final injection.

3.2.1.4 Tissue collection

The mice were anaesthetised with Isoflurane and sacrificed through cervical dislocation. Blood was collected by cardiac puncture, and remnant livers were fixed in 4% PFA or snap-frozen in liquid nitrogen immediately after explantation and stored at -80°C until further use. Serum was collected by centrifuging blood at a speed of 7,000 rpm for 7 minutes and stored at -80°C until further use.

3.2.2 Liver function test

Serum samples were collected as mentioned. The serum level of alanine transaminase (Schulze, Stoss et al.) was measured using an ELISA kit according to the manufacturer's instructions as follows:

- The wells were determined for diluted standard, blank and sample. 100μL each of dilutions of standard, blank and samples were added into the wells. The plate was covered with the plate sealer and then incubated for 1 hour at 37°C.
- The liquid was removed of each well.
- 100μL of Detection Reagent A working solution were added to each well. The plate was covered with the plate sealer and then incubated for 1 hour at 37°C.
- The solution was aspirated and each well was washed with 350μL of 1× Wash Solution using an autowasher for 3 times.
- 100μL of Detection Reagent B working solution were added to each well. The plate was covered with the plate sealer and then incubated for 30 minutes at 37°C.
- The solution was aspirated and each well was washed with 350μL of 1× Wash Solution using an autowasher for 5 times.
- 90μL of the Substrate Solution was added to each well. The plate was covered with the plate sealer and then incubated for 20 minutes at 37°C, protected from light.
- 50μL of Stop Solution was added to each well. The liquid was mixed by tapping the side of the plate.
- Water was removed and there were no bubbles on the surface of the liquid. Then, the conduct measurement at 450nm was running by the microplate reader immediately.
- The results was calculated according to standard curve.

3.2.3 DNA related methods

3.2.3.1 DNA isolation

A 0.5cm piece of mice tail was cut for DNA isolation. First, tails were digested in 500 µl Sodium Chloride-Tris-EDTA(STE) buffer and 25µl proteinase K in a 55 °C incubator overnight (550rpm). After incubation, the samples were centrifuged at 12000rpm for 10 minutes, and the supernatant was transferred into new tubes with 400 µl of isopropanol to precipitate the DNA. After 10 minutes of incubation at room temperature, the samples were centrifuged at 12000rpm at room temperature again, the supernatant was discarded and the remaining DNA pellets were washed with 500ul 70% ethanol twice. After each wash the samples were centrifuged at 12000rpm at room temperature for 10minutes. The tubes were dried in a 37 °C incubator at least for 10minutes; afterwards, 50 µl Dnase-free water was added to resuspend the DNA. The DNA samples were stored at 4°C until use.

STE buffer	
NaCl	0.1 M
Tris-Hcl	10 mM
EDTA	1 mM
SDS	1 %
pH	8
Aqua dest	various

3.2.3.2 Genotyping

The transgenes Brg1 and Alb-Cre were detected by polymerase chain reaction (PCR) with specific pairs of primers according the following protocols.

Reaction mix	
PCR Master Mix, 2x	12.5 µl

Sense primer (10 µM)	0.5 µl
Antisense primer (10 µM)	0.5 µl
DNA template	1 µl
RNase-free water	10.5 µl
Total volume	25 µl

Primer sequences:

Brg1

Primer name	Sequence
TH185	GTC ATA CTT ATG TCA TAG CC
TG57	GCC TTG TCT CAA ACT GAT AAG

AlbCre

Primer name	Sequence
Transgene forward	GCG GTC TGG CAG TAA AAA CTA TC
Transgene reverse	GTG AAA CAG CAT TGC TGT CAC TT
Internal positive control forward	CTA GGC CAC AGA ATT GAA AGA TCT
Internal positive control reverse	GTA GGT GGA AAT TCT AGC ATC ATC C

PCR programs

Procedure	Temperature	Duration
1. Starting	94 °C	1 minute
2. Denaturation	94 °C	30 seconds
3. Annealing	58 °C	30 seconds
4. Elongation	72 °C	60 seconds

40 cycles for 2-4 steps

5. Elongation	72 °C	10 minutes
6. Conservation	4 °C	

3.2.4 RNA-related methods

3.2.4.1 RNA isolation

Total RNA was extracted from collected mouse liver tissue with an RNeasy Plus Mini Kit (Qiagen) according to the manufacturer's instructions.

- Around 30 mg of mouse liver tissue was placed in 350 µL RLT Plus with 0.35 µL β-ME. The lysate was homogenised and then centrifuged for 3 minutes at maximum speed. The supernatant was carefully collected, and the rest was discarded.
- The homogenised lysate was transferred to a gDNA Eliminator spin column placed in a 2 ml collection tube and centrifuged for 30 seconds at ≥8000 x g (≥10,000 rpm). The column was discarded and flow-through was saved.

- One volume of 70% ethanol was added to the lysate and mixed by pipetting. Up to 700 µl of the sample, including any precipitate, was transferred to an RNeasy spin column placed in a 2 ml collection tube and centrifuged for 15 seconds at 8000 x g. The flow-through was discarded.
- Then, 700 µl Buffer RW1 was added to the column. The lid was closed, and the sample was centrifuged for 15 seconds at 8500 x g. The flow-through was discarded.
- Next, 500 µl Buffer RPE was added to the RNeasy spin column. The lid was closed, and the contents were centrifuged for 15 seconds at 8000 x g. The flow-through was discarded.
- Afterwards, 500 µl Buffer RPE was added to the RNeasy spin column. The lid was closed gently, and the contents were centrifuged for 2 minutes at 8000 x g. Then, the RNeasy spin column was placed in a new 2 ml collection tube

and centrifuged at full speed for 1 minute to dry the membrane.

- The RNeasy spin column was placed in a new 1.5 ml collection tube. Next, 50 µl RNase-free water was added to the spin column membrane. The lid was closed, and the contents were centrifuged for 1 minute at 8500 x g to elute the RNA.
- The RNA samples were stored in the fridge at −80 °C.

3.2.4.2 Evaluation of RNA quality and cDNA synthesis

The RNA concentrations were tested using the NanoDrop. The absorbance proportion at 260 nm and 280 nm wavelengths was used to evaluate the RNA's quality. A ratio of around 2.0 was recommended as pure RNA.

The RNA was reverse-transcribed with the QuantiTect Reverse Transcription Kit. The steps are as follows.

- Eliminate genomic DNA in RNA.

Component	Volume
Template RNA, up to 1µg	variable
RNase-free water	variable
gDNA wipeout buffer,7x	2 µl
Total volume	14 µl

- The reaction mix incubated for 2 minutes at 42 °C being investigated, and afterwards put on ice immediately.
- Then, the reverse-transcription master mix was prepared as follows on ice.

Component	Volume
Genomic DNA elimination reaction mix	14 µl
Quantiscript Reverse Transcriptase	1µl

Quantiscript RT buffer, 5x	4 µl
RT primer mix	1 µl
Total volume	20 µl

- The reaction mix was incubated for 15 minutes at 42°C and then incubated for 3 minutes at 95°C to inactive Quantiscript reverse transcriptase. The final cDNA concentration was adjusted and stored at −20°C.

RNA levels were normalized to those of GADPH and were depicted as a fold difference relative to liver samples of untreated mice. The accumulation of PCR amplicons was quantified on a LightCycler 480 Real-Time PCR system.

3.2.4.3 Quantitative real-time PCR

Quantitative real-time PCR (qRT-PCR) was carried out using a LightCyclerTM480 system with the SYBR Green Master Kit. The cycle threshold (CT) value described the cycle of the PCR in which the fluorescence signal became significant.

qPCR reaction mix

SYBR Green Super Mix	10 µl
Primers	2 µl
cDNA template	5 µl
ddH_2O	3 µl
Total	20 µl

qPCR reaction program

Procedure	Temperature	Duration
1. Pre-incubation	95 °C	5 minutes
2. Denaturation	95 °C	15 seconds
3. Annealing	50 °C	15 seconds
4. Elongation	72 °C	15 seconds

45 cycles for 2– 5 steps		
6. Melting curve	95°C	1 second
	65°C	20 seconds
	98°C	continuous
7. Cooling	40°C	30 seconds

3.2.4.5 RNAseq analysis

RNA was prepared using the RNeasy Mini Kit. Library preparation for bulk 3'-sequencing of poly(A)-RNA was done as described previously (Parekh, Ziegenhain et al. 2016). Briefly, the barcoded cDNA of each sample was generated with a Maxima RT polymerase (Thermo Fisher) using oligo-dT primer containing barcodes, unique molecular identifiers (UMIs), and an adapter. The 5' ends of the cDNAs were extended by a template switch oligo (TSO) and full-length cDNA was amplified with primers binding to the TSO-site and the adapter. cDNA was tagmented with the Nextera XT kit (Illumina) and 3'-end-fragments finally amplified using primers with Illumina P5 and P7 overhangs. In comparison to Parekh et al. the P5 and P7 sites were exchanged to allow sequencing of the cDNA in read1 and barcodes and UMIs in read2 to achieve a better cluster recognition. The library was sequenced on a NextSeq 500 (Illumina) with 75 cycles for the cDNA in read1 and 16 cycles for the barcodes and UMIs in read2.

Annotations and the reference genome from the Gencode release M15 were derived from the Gencode homepage *(https://www.gencodegenes.org/)*. The Dropseq tool v1.12 was used for mapping the raw sequencing data to the reference genome. The resulting UMI filtered count matrix was imported into R v3.4.4 and differential gene expression analysis was conducted with DESeq2(Love, Huber et al. 2014). A gene was called differentially expressed if the adjusted p-value was below 0.05 and the absolute log2 fold change was 0.7. Pathway analysis was conducted with EnrichR(Kuleshov, Jones et al.

2016), within the Reactome database. Pathways with an FDR-level of 0.05 were considered to be statistically significant. Gene level differences for genes being regulated between time points and located in selected pathways are shown as a heatmap.

GSEA analysis was performed with a pre-ranked gene list. The rank of a gene was determined according to the following formula:

$\mathrm{Rank}(gene_i) = -log_{10}\,\mathrm{pvalue}(gene_i) \times log_2\mathrm{FoldChange}(gene_i)$ for all genes i..n

Gene Set Variation Analysis was performed with the Bioconductor Package GSVA v1.28.0 (Hanzelmann, Castelo et al. 2013) after rlog transformation of the UMI filtered Countmatrix within DESeq2. The GSEA Hallmark geneset from the MsigDB database v6.2 was downloaded from *http://software.broadinstitute.org/gsea/msigdb/index.jsp* and was used as input for GSVA. The resulting pathway scores were tested with a ranked based ANOVA for association with the genotype at timepoint 48 hours. P-values were adjusted with the Benjamini Hochberg procedure. We consider a geneset to be positively associated with a genotype at an FDR level of 0.1. The Z-score transformed scores for pathways associated with genotype are displayed as a heatmap.

This part of the work was supported by Thomas Engleitner, Rupert Öllinger and Roland R. Rad from Institute of Molecular Oncology and Functional Genomics, Department of Medicine II and TranslaTUM Cancer Center, Klinikum rechts der Isar, Technical University of Munich, Munich, Germany.

3.2.5 Western blot

3.2.5.1 Protein extraction from liver tissue

A piece of frozen liver tissue weighing 50 mg was lysed in 350 µl RIPA buffer supplemented with protease and phosphatase inhibitors. Then, the tissue was disrupted with a homogeniser for 5 minutes. Afterwards, the sample was put on ice for 40 minutes and then centrifuged at full speed for 20 minutes at 4°C. The supernatant was taken carefully and kept at −80°C until use.

3.2.5.2 Protein concentration measurement

Protein concentration was determined by using the Pierce™ BCA Protein Assay Kit. BCA reagent was freshly prepared by adding 4% $CuSO_4$ to the standard solution and protein solution at a ratio of 1:50. Then, 5 µl of the probe or the standard solution was added to a microtiter 96-well plate and mixed with 200 µl of the prepared BCA solution. After being incubated at 37°C for 25 minutes, the extinction was measured at a wavelength of 560 nm and the protein concentration was calculated.

3.2.5.3 Protein denaturation

The protein denature mix was prepared as follows.

Protein denature mix

Protein	variable (up to 20µg)
Water	39 µl-volume of protein
NuPAGE LDS Sample Buffer 4x	15 µl
NuPAGE Reducing Agent 10x	6 µl
Total volume	60 µl

The mixture was denatured at 70°C for 10 minutes and used directly or kept at −20°C until use.

3.2.5.4 SDS-polyacrylamide gel electrophoresis (SDS-PAGE)

The protein samples were separated according to their size by using a discontinuous gel system, which involved stacking (5%) and separating gel (7.5-12%) layers that differed in their salt and acrylamide concentrations. Twenty micrograms of protein from each sample was loaded into suitable polyacrylamide gel and separated by gel electrophoresis in running buffer (25 mM Tris, 192 mM glycine, 0.1% SDS, pH 8.3) at 60V until the samples were focused in the stacking gel, and then the gel was run at 100 V until the target band was at the right position.

Separating gel (for 2gels)	
ddH2O Acrylamide 30%	7.4ml
Tris-HCL 1.5M pH8.8	2.6ml
SDS 10%	100µl
APS 10%	50µl
Temed	15µl
Total	10ml

Stacking gel (4% for 2 gels)	
ddH2O	3ml
Acrylamide 30%	750µl
Tris-HCL 1.5M pH6.8	1.3ml
SDS 10%	50µl
APS 10%	25µl
Temed	10µl
Total	5ml

3.2.5.5 Immunoblotting

When the target band arrived at the appropriate position, proteins were transferred electrophoretically onto a nitrocellulose blotting membrane using a Trans-Blot SD Wet Transfer Cell. The transfer conditions were 250 mA for 1-2 hours at room temperature, depending on the molecular weight of the target protein. Then, the membrane was blocked with 5% nonfat milk or BSA for 1 hour. Afterwards, membranes were incubated with the primary antibodies diluted with blocking solution overnight at 4°C.

On the second day, the membrane was washed with TBST (Tris-buffered saline with 0.1% Tween 20) three times for 10 minutes each. Then, the membrane was incubated with Secondary antibody goat-anti-rabbit-HRP or goat-anti-mouse-HRP (Promega) diluted with 5% nonfat milk for 1hour at room temperature. Afterwards, the membrane was washed again with TBST three times for 10 minutes each.

Then Antibody binding was visualised using the Pierce™ ECL western blotting detection system. The blots were exposed to an autoradiography film. Densitometric analysis was performed using the ImageJ software *(https://imagej.nih.gov/ij/)*.

3.2.6 Histology and immunohistochemistry

3.2.6.1 Paraffin sections

- After fixation with 4% PFA for 48 hours, the tissues were trimmed and fixed into appropriate sizes and shapes, before being placed in embedding cassettes.
- The samples went through ascending alcohol rows to dehydrate, using an automatic tissue processor.
- The tissue samples were embedded into paraffin blocks.
- After cooling them down to -15 °C, the blocks were cut into 3 µm sections.

- The sections were moved to an incubator for drying at 37°C overnight.

3.2.6.2 Hematoxylin and eosin staining

- Paraffin-embedded tissue sections were deparaffinised with Roticlear three times for 10 minutes each.
- Samples were rehydrated in an descending row of alcohol (3x 2 minutes 100% ethanol; 1 x 2 minutes 96% ethanol; 1 x 2 minutes 70% ethanol; 1 x 2 minutes 50% ethanol). The slides were stained in hematoxylin solution for 30 seconds and washed in running tap water for at least 15 minutes.
- The slides were counterstained in eosin for 5 seconds.
- They were washed in tap water shortly and then dehydrated in a descending row of alcohol(1 x 5 seconds 70% ethanol,1x 0.5 minute 96% ethanol; 3 x 2 minutes 100% ethanol), with a final immersion in Roticlear three times, for 10 minutes each. The slides were mounted with mounting medium and sealed with a coverslip.

3.2.6.3 Sirius red staining

- De-wax and hydrate paraffin sections.
- Stain in sirius red solution for one hour.
- Wash in three changes of acidified water (4minutes -> 14minutes-> 17minutes).
- Physically remove most of the water from the slides by vigorous shaking or (for a few slides only) blotting with damp filter paper.
- Dehydrate in three changes of 100% ethanol(2 minutes per change).
- Clear in xylene and mount in a resinous medium.

Sirius red Solution

Saturated aqueous solution of picric acid (5.5g)	500 ml

Sirius red F3B (C.I. 35782)	0.5g

Acidified Water

Add 5 ml acetic acid (glacial) to 1litre of water (tap or distilled).

3.2.6.4 Immunohistochemistry staining

Immunohistochemistry staining was performed with the Dako Envision System.

- Paraffin-embedded tissue sections were deparaffinised with Roticlear three times for 10 minutes each. Then, samples were rehydrated in a descending row of alcohol (3x 2 minutes 100% ethanol; 1 x 2 minutes 96% ethanol; 1 x 2 minutes 70% ethanol; 1 x 2 minutes 50% ethanol).
- Antigen retrieval was performed by retreating the slides in citrate buffer (pH 6.0; 10 mM citric acid) in a 600W microwave oven for 15 minutes. Then, the slides were put on a bench for at least 30 minutes to cool down.
- The slides were washed in Tris-buffered saline (TBS) with 0.1%BSA for 5 minutes and blocked with 3% H_2O_2, which was diluted with absolute methanol for 10 minutes in the dark. Slides were then washed again in TBS/0.1% BSA 3 times, for 5 minutes each time.
- The reaction was blocked with TBS/10% goat serum for 1 hour at room temperature.
- The primary antibodies were diluted to recommended concentrations in blocking solution, pipetted onto the slides and incubated overnight at 4°C in a humidified slide chamber.
- The slides were rinsed three times, for 10 minutes each time, with TBS/0.1% BSA and incubated with secondary antibody for 1 hour at room temperature.
- The slides were washed with TBS/0.1% BSA three times, for 10 minutes each time. Then, an enzymatic reaction with substrate solution (0.5 mg DAB/phosphate buffer) was performed in the slides. The reaction was

stopped in water when it was ready.

- The slides were stained in hematoxylin solution for 3 seconds and washed in running tap water for at least 15 minutes.
- The tissue was dehydrated in an ascending alcohol row (1 x 2minutes 50% ethanol, 1 x 2minutes 70% ethanol, 1x 2 minutes 96% ethanol, 3 x 2minutes 100% ethanol) and cleared in Roticlear three times, for 10 minutes each.
- Finally, the slides were mounted with mounting medium and sealed with a coverslip.

For qualification, five random high power fields were counted and the fraction of stained hepatocyte nuclei was calculated for each animal.

3.2.6.5 Immunofluorescence staining

Deparaffinization and rehydration of paraffin sections (3 µm) was performed according to standard protocols. Antigen retrieval was carried out with epitope retrieval solution at pH 6. The first antibody was incubated overnight at 4°C, The secondary antibody was applied for 1 hour at room temperature after three washing steps with PBS. Sections were mounted with Dako fluorescent mounting medium and photographed with ECLIPSE Ni-E microscope. This part of work was supported by Victor Olsavszky and Cyrill Geraud from Department of Dermatology, Venereology, and Allergology, University Medical Center and Medical Faculty Mannheim, Heidelberg University and Center of Excellence in Dermatology, Mannheim, Germany.

3.2.7 Statistical analysis

Statistical analysis was performed using the GraphPad Prism software (5.0a; Graph- Pad Software, Inc., San Diego, CA). Variation is always indicated by using the standard error presented as mean ± SEM. Continuous data were tested for normality and analysed by Unpaired Student's *t*-tests,

Mann-Whitney *U* test or one-way ANOVA, as appropriate. Statistical significance is displayed as $p < 0.05$ (*), $p < 0.01$ (**) or $p < 0.001$ (***) unless specified otherwise. In all experiments, no mice were excluded from analysis after the experiment was initiated. Image analysis for the quantification of cell proliferation was blinded.

4 RESULTS

4.1 Brg1 knockout mice show normal liver development

Hepatocyte-specific Brg1 knockout mice (AlbCre-Brg1$^{fl/fl}$ mice, termed Brg1 KO mice in the following) were generated by breeding Brg1-floxed mice with albumin-Cre transgenic (AlbCre) mice, which express Cre recombinase, specifically in hepatocytes under the control of the albumin promoter (Postic, Shiota et al. 1999). Brg1$^{fl/fl}$, Brg1$^{fl/-}$ mice obtained from the same litter were used as the control group (in the following termed Control mice).

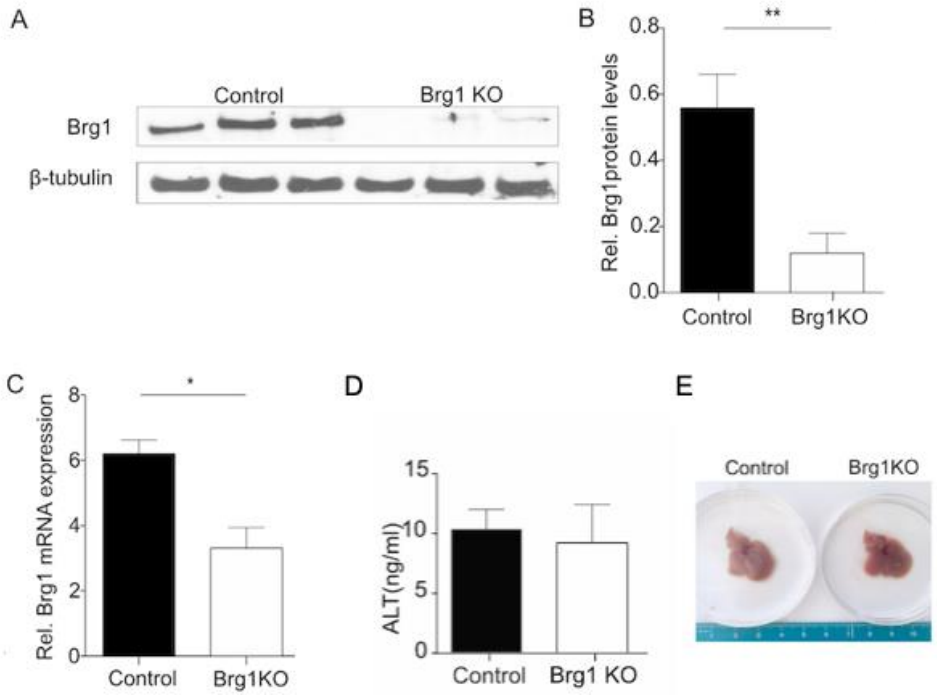

Figure 4. Brg1 hepatocyte-specific knockout mice model
(A, B) Protein expression of Brg1 in the liver of 2-month-old Control and Brg1 KO mice analysed by Western blot. Representative gels (A) and densitometric analyses (B) are depicted, n=3. (C) mRNA expression of Brg1 of 2-month-old Control and Brg1 KO mice in the liver analysed by qPCR, n=3. (D) ALT level of Brg1 KO and Control mice (E) Representative liver morphology of 2-month-old Control and Brg1 KO mice.

For the following analysis, the livers of 2-month-old Brg1 KO mice and Control mice were compared. In the liver tissue, Brg1 KO mice showed a significant

decrease of about 80% of the protein and RNA expression of Brg1 compared to Control mice (Fig. 4A-C). Since the albumin promoter is active in hepatocytes but not in other liver cells, non-hepatocytes expressed Brg1 in liver tissue of Brg1 KO mice (Fig. 5B).

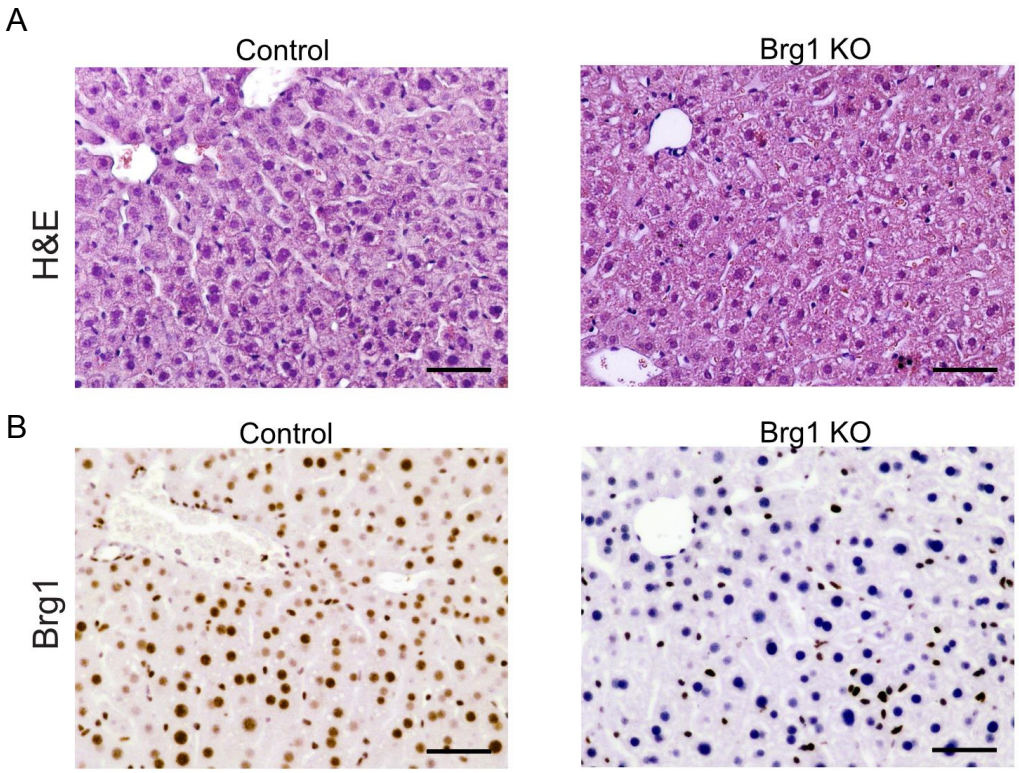

Figure 5. Histology of Control and Brg1 KO mice
(A) H&E staining of the liver of 2-month-old Control and Brg1 KO mice. (B) Immunohistochemistry for Brg1 of the liver of 2-month-old Control and Brg1 KO mice (bar = 100 μm).

Brg1 KO mice were healthy and possessed normal transaminase levels (Fig. 4D-E). Liver structure and metabolic zonation were similar in both the Brg1 KO and Control groups (Fig. 5A, Fig. 6A-C). Glutamine synthetase (GS) and Rh Family B Glycoprotein (Rhbg) show staining pattern in pericentral hepatocytes and Arg1 in the periportal hepatocytes. Liver endothelial cells show a zonated expression pattern as well, with Endomucin (EMCN) in pericentral liver sinusoidal endothelial cells (LSECs) and central vein endothelial cells (CVECs), and LYVE1 in midzonal LSECs (Leibing, Geraud et al. 2018).

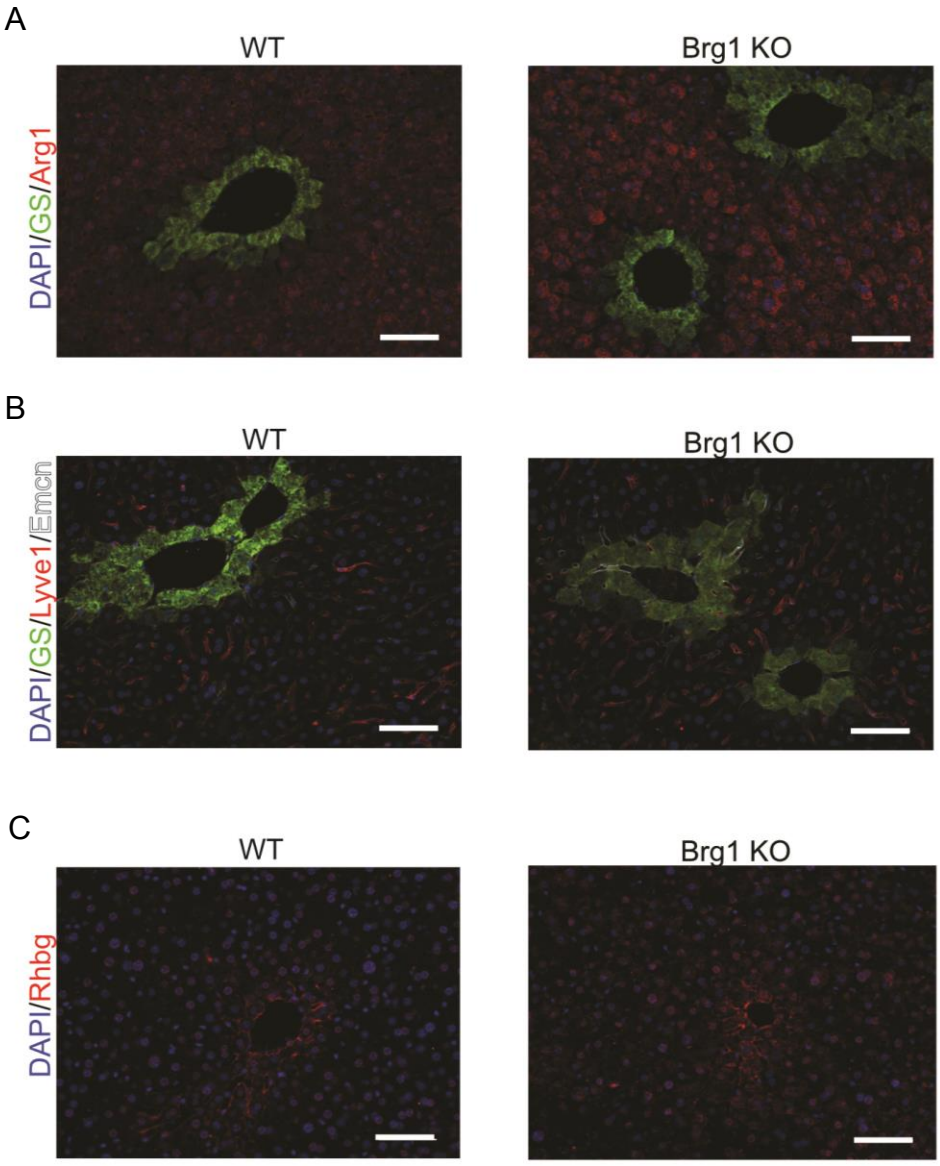

Figure 6. Liver metabolic zonation in Brg1 KO and Control groups
(A-C) Representative immunofluorescence images for Glutamine synthetase (GS)/Arginase-1 (Arg-1), GS/Lymphatic vessel endothelial hyaluronan receptor 1 (Lyve1)/Endomucin (Emcn) and Rh Family B Glycoprotein (Rhbg) of the liver of 2-month-old Control and Brg1 KO mice, n=3(bar = 100 μm). Cell nucleus was dyed by DAPI.

The body weight, liver weight, and the liver to body weight ratio of Brg1 KO mice were not significantly different from those of Control mice (Fig. 7A-C). The proliferation rate and hepatocyte cell size in the liver tissue of 2-month-old

Brg1 KO and Control mice were compared by BrdU staining (Fig. 7E). Neither the proliferation ratio nor hepatocyte cell size were significantly different in Brg1 KO mice compared to Control mice (Fig. 7D, 11B).

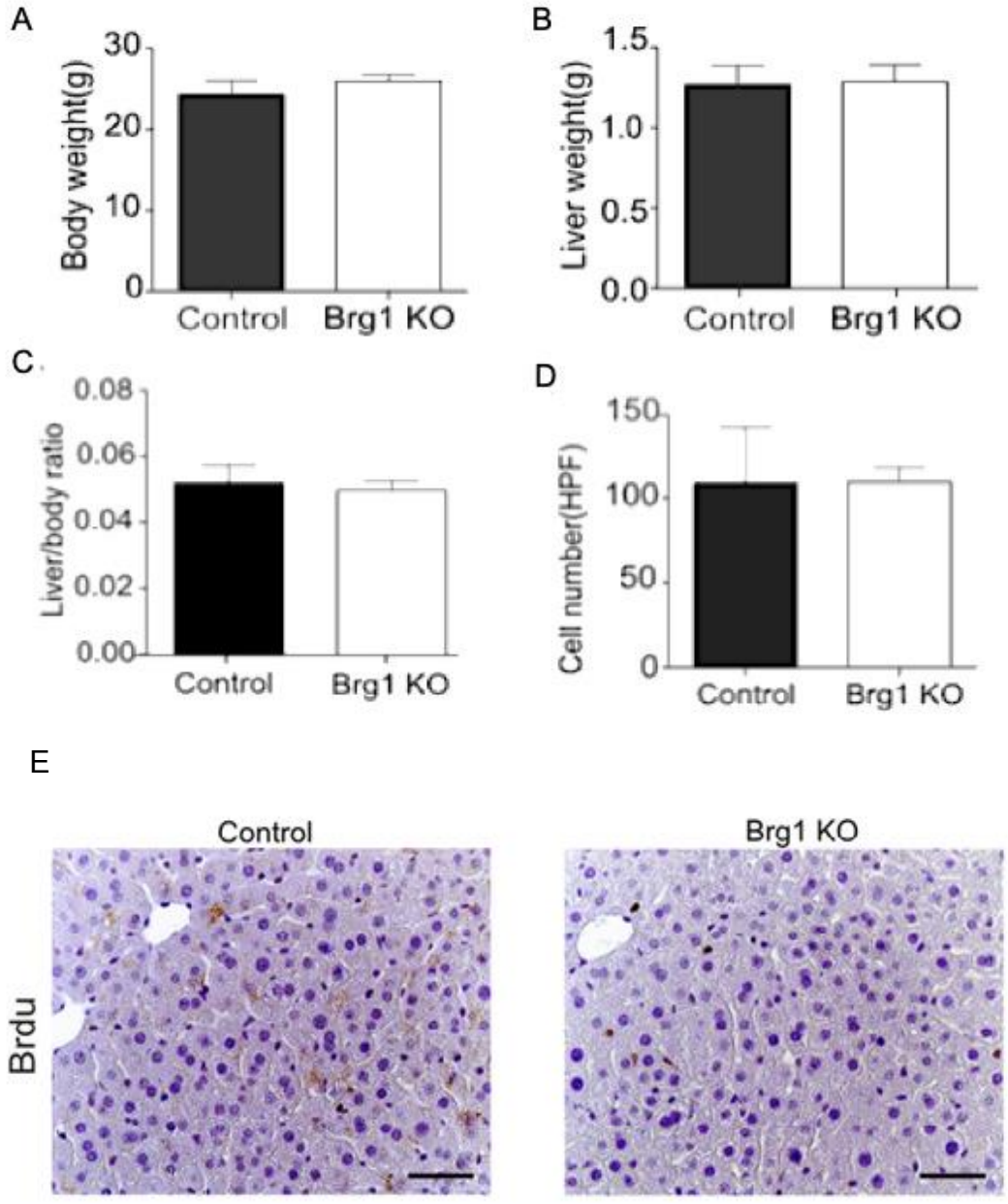

Figure 7. Brg1 knockout mice show normal liver development

(A,B) Liver weight and body weight of 2-month-old Control and Brg1 KO mice, n=6. (C) Liver to body weight ratios of 2-month-old Control and Brg1 KO mice, n=6. (D) Quantification of cell number (HPF) of 2-month-old Control and Brg1 KO mice, n=6. (E) Representative immunohistochemistry images for BrdU of 2-month-old Control and Brg1 KO mice livers(bar = 100 μm).

4.2 Brg1 promotes liver regeneration after partial hepatectomy via the regulation of the cell cycle

4.2.1 Brg1 expression increases after PH

Hepatic Brg1 expression was assessed, before and at different time points after PH in mice to explore the regulation of Brg1 during liver regeneration. Weak Brg1 expression was observed in the healthy liver before PH. In the early stage of liver regeneration (within 24h after PH), there was no significant alteration of the Brg1 expression on mRNA or protein levels (Fig. 8 A-C).

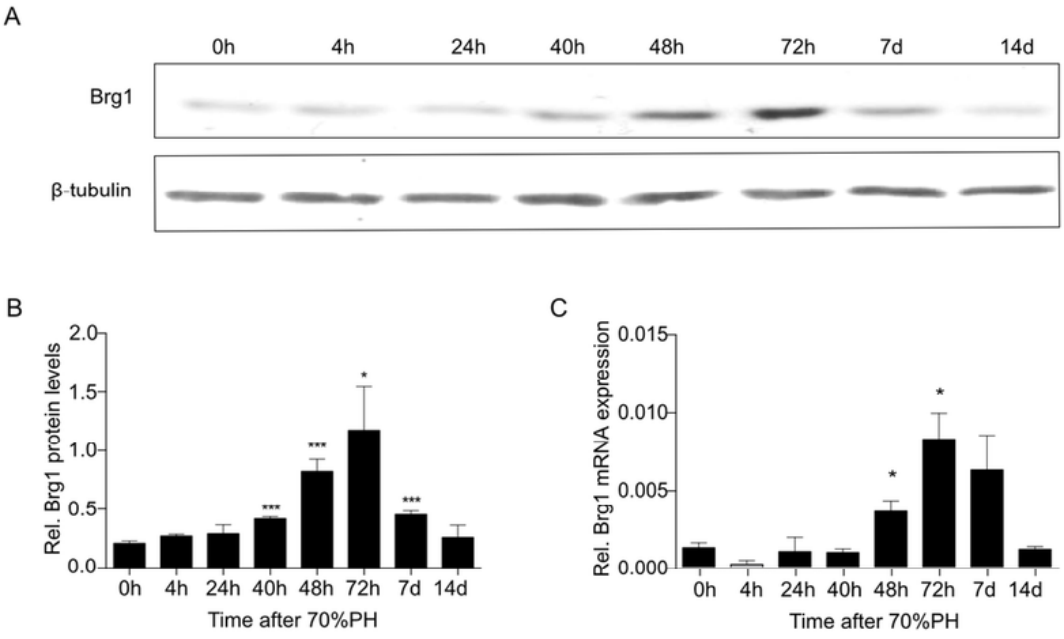

Figure 8. Brg1 expression during liver regeneration after PH in mice
(A, B) Protein expression of Brg1 in the liver after PH analysed by Western blot. Representative gels (A) and densitometric analyses (B) are depicted, n=3. (C) mRNA expression of Brg1 after PH, n=3.

Both the protein and mRNA levels of Brg1 started to increase gradually when liver regeneration proceeded. Three days after PH, the highest level of protein and mRNA expression of Brg1 was measured (Fig. 8 A-C). At day 2 after PH, Brg1 protein expression was increased by approximately 4.0-fold; at day 3

after PH, Brg1 protein expression was increased by approximately 6.3-fold compared to the protein level before PH. After a peak of Brg1 expression on day 3 after PH, Brg1 expression on day 7 declined to equalise the expression level seen before PH.

4.2.2 Brg1 loss impairs liver regeneration after PH

To investigate the role of Brg1 in liver regeneration, a surgical resecting of two-thirds of the liver was performed. After liver resection, the liver tissues of both Brg1 KO and Control mice were vital and exhibited neither necrosis nor inflammation analysed by H&E staining (Fig. 9A).

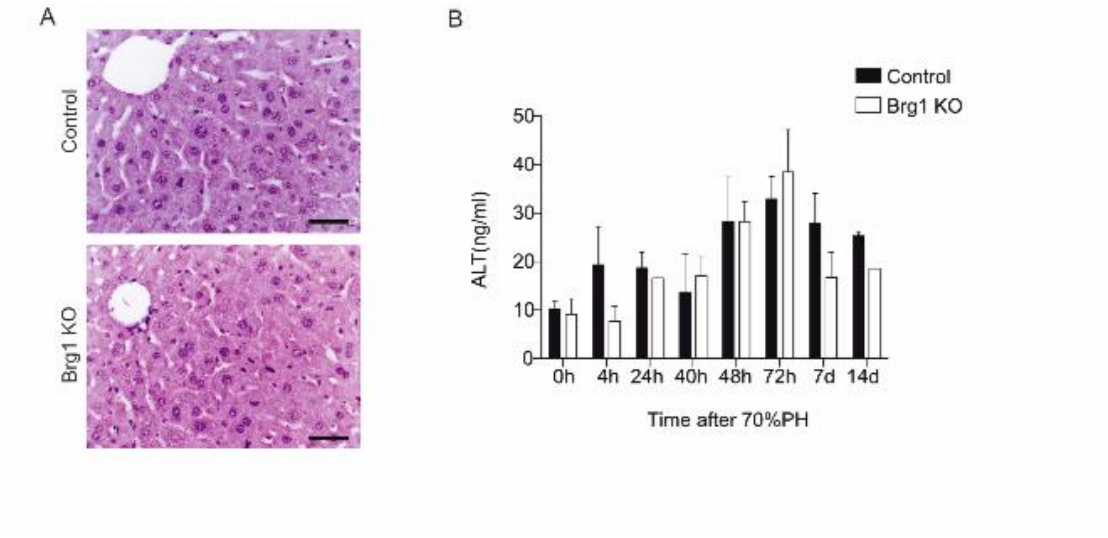

Figure 9. Brg1 deletion does not impact liver injury during liver regeneration after PH in mice
(A) Representative H&E staining of Control and Brg1 KO mice at 40h after PH (bar = 100 μm). (B) ALT levels were measured using serum samples of post-PH Control and Brg1 KO mice, n>4.

Liver regeneration was markedly impaired in Brg1 KO mice, showing a significantly reduced liver to body weight ratio and liver weight at 48h, 72h, 168h, and 336h after PH compared to Control mice (Fig. 10A-C). Concerning the liver to body weight ratio and liver weight, the liver regeneration of Control mice was nearly completely terminated 168h after PH, whereas Brg1 KO mice showed a prolonged time for recovery of the same liver mass that even after

336h did not reach the levels of Control mice at 168h (Fig. 10A-C). Increased levels of ALT indicate liver cell injury. ALT levels strongly increased after PH in both Brg1 KO and Control mice, but no significant difference of ALT expression was seen between the phenotypes (Fig. 9B).

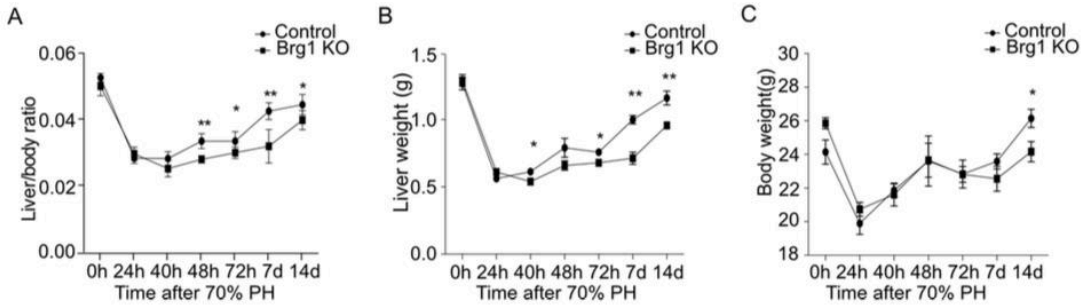

Figure 10. Lack of Brg1 delays recovery of liver tissue after PH
(A) Liver to body weight ratios, (B) liver weight and (C) body weight were determined at the indicated time points after PH, n=6.

Extensive proliferation of liver parenchymal cells is required to restore liver tissue (Michalopoulos 2017). In order to analyse proliferation, the staining of Ki67 as a marker for the mid-G1 phase to the end of mitosis and incorporation of 5-bromo-2'-deoxyuridine (BrdU) for the S phase were performed. Analysing both BrdU and Ki67 immunoreactivity, active proliferation was observed in hepatocytes in Control mice from 40h to 48h post-PH, while proliferation was significantly decreased in Brg1 KO mice at these time points (Fig. 11A, B).

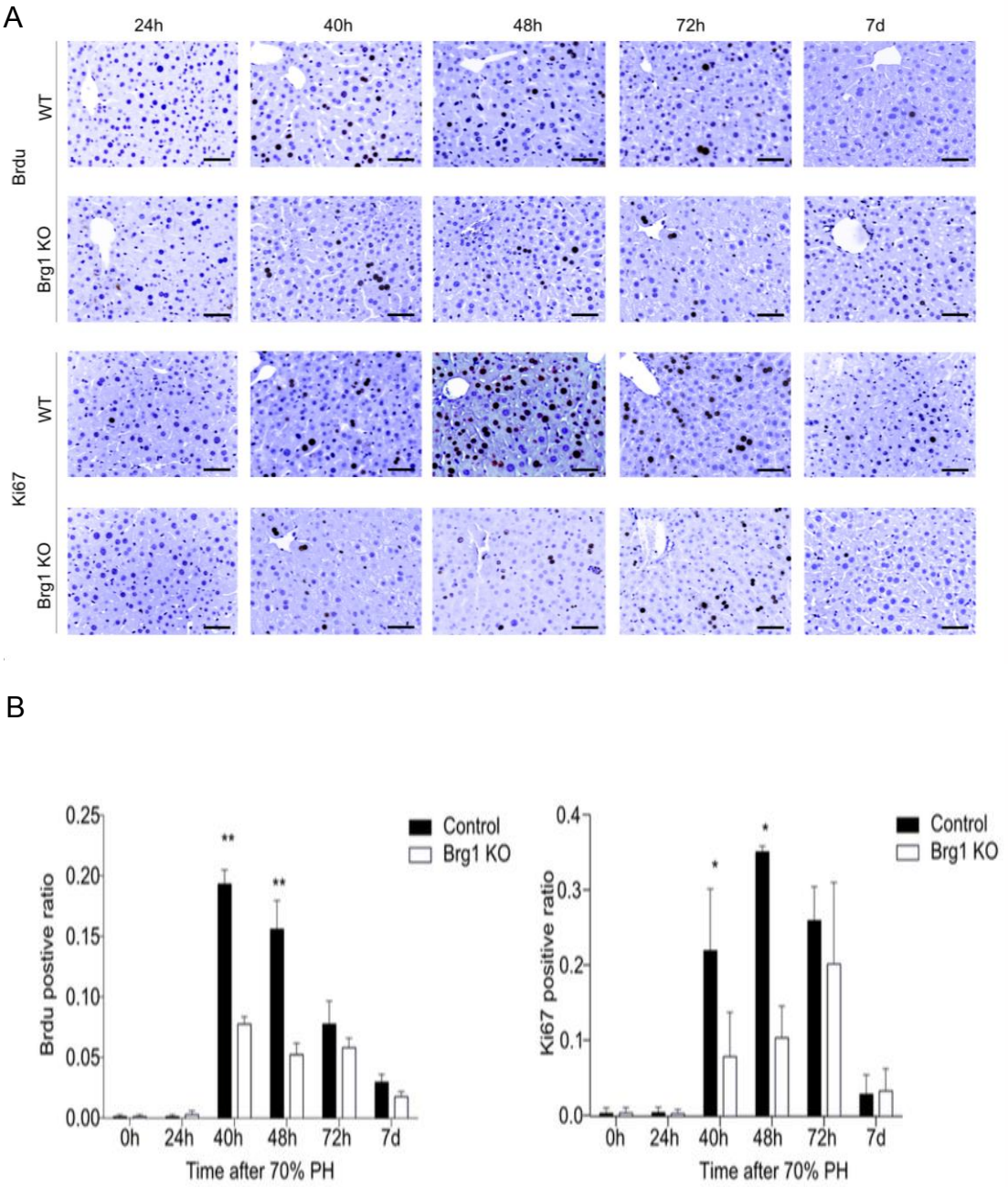

Figure 11. Lack of Brg1 impairs liver proliferation after PH

(A) Representative immunohistochemical images for BrdU and Ki67 at the indicated time points (bar = 100 μm). (B) Quantification of positive staining of BrdU and Ki67 in hepatocyte nuclei at the indicated time points, n=6.

The cell cycle-dependent proliferating cell nuclear antigen (PCNA) expression is commonly used as an accurate and reproducible marker of liver regeneration, whereas phosphorylated histone H3 (pH3) is a G2/M marker. Therefore, the protein expression of PCNA and pH3 was evaluated by

Western Blot (WB). In line with the results from the Ki67 and Brdu staining, it was shown that in the expression of PCNA and pH3 was significantly lower than in the Control group at 40h after PH for both PCNA and pH3 and at 48h after PH for pH3 (Fig. 12A-C). Taken together, these results demonstrate that Brg1 is required for adequate hepatocyte proliferation during recovery of liver tissue after PH.

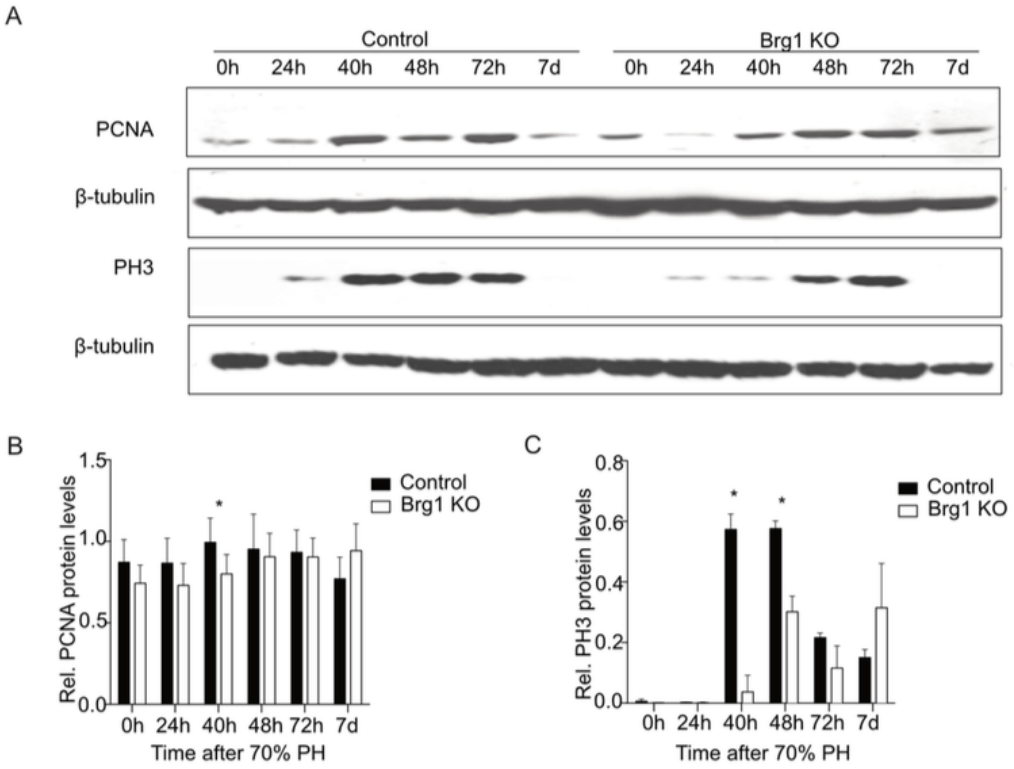

Figure 12. The expression of PCNA and PH3 of Control and Brg1 KO group after PH
(A-C) Analysis of protein expression of PCNA and PH3 in the liver by Western blot. Representative gels (A) and densitometric analyses (B, C) are depicted, n>3.

4.2.3 Loss of Brg1 impairs liver regeneration by modulating the cell cycle pathway

To identify genes regulated by Brg1 during liver regeneration, RNA-sequencing (*RNA-seq)* on liver extracts was performed. Four time points (4h, 24h, 40h and 48h) post-PH were screened and these expression levels were compared to the baseline expression pre-PH.

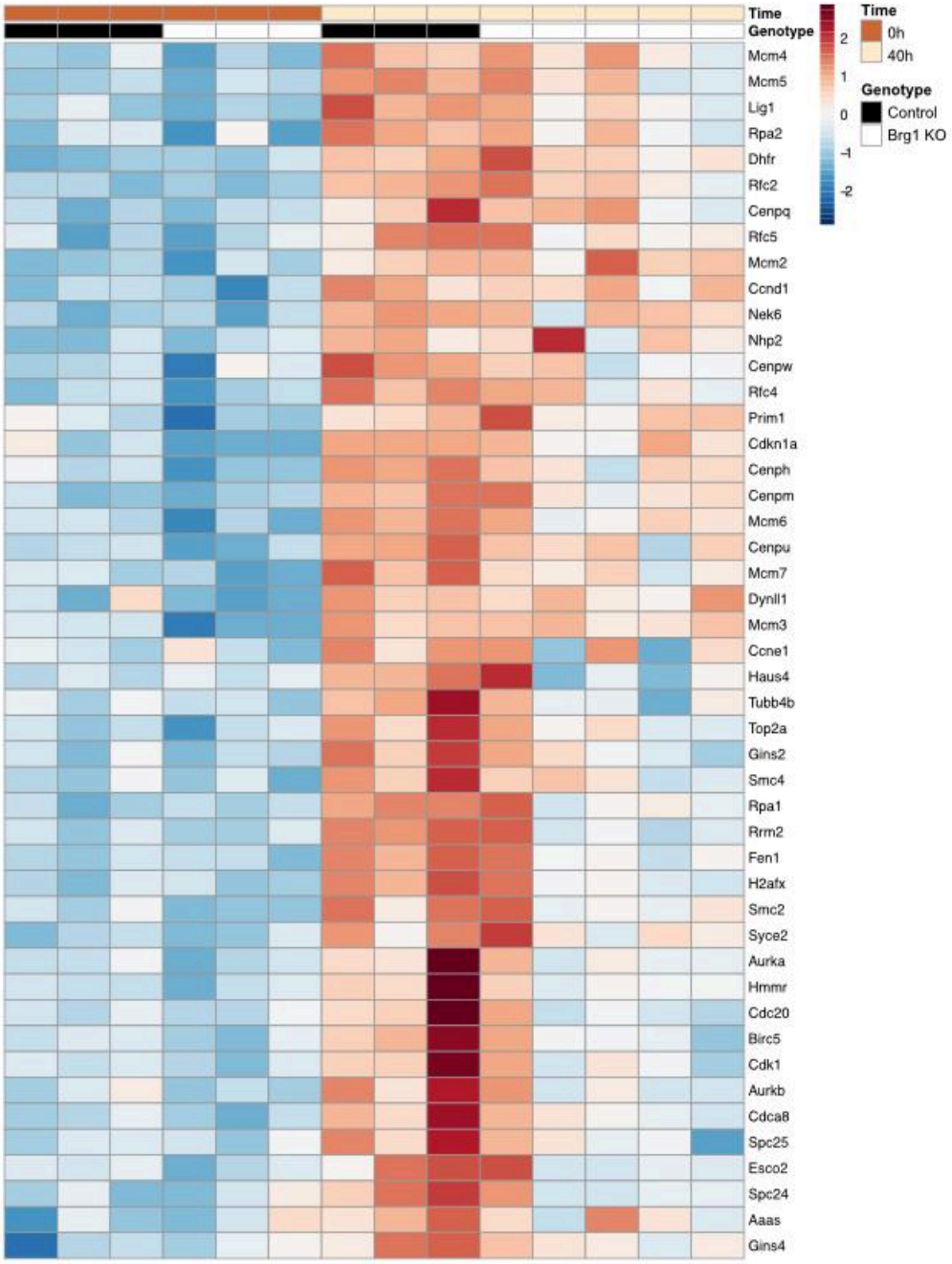

Figure 13. Loss of Brg1 impairs liver regeneration by modulating the cell cycle pathway

A heatmap of significantly regulated cell cycle related genes. The the z-scaled gene expression for genes, being significantly regulated between the time points 0h and 40h, within both the Control and Brg1 KO group, and overlap with the cell cycle pathway annotation from Reactome. The colour scale represents the z-scaled gene expression levels. Red colour corresponds to up-regulated genes and blue colour corresponds to down-regulated genes.

At time points 40h and 48h, both Brg1 KO group and Control group showed an upregulation of genes related to the cell cycle pathway, such as Ccnb1, Ccnb2, Cdk1 and Cdc20. Interestingly, this regulation is much less pronounced in the Brg1 KO group compared to the Control group (Fig. 13).

In accordance with this observation, a Gene Set Enrichment Analysis (GSEA) analysis for differences between genotypes at time point 48h also shows a significant downregulation of the cell cycle pathway in the Brg1 KO group (Fig. 14A).

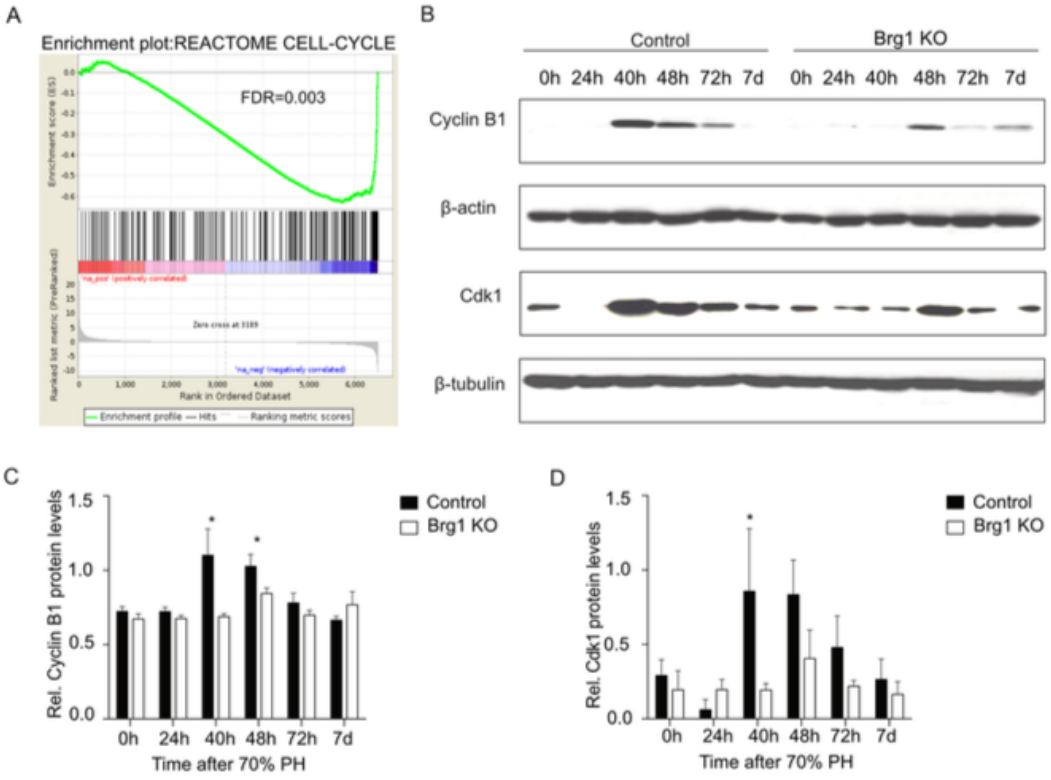

Figure 14. Loss of Brg1 impairs cell cycle progression in mice
(A) GSEA enrichment plot for the cell cycle pathway. GSEA analysis was conducted for detecting differences between the Brg1 KO and the Control group at 48h post PH. The cell cycle pathway is significantly associated with the Brg1 KO genotype (FDR = 0.0003). (B-D) Protein expression of Cyclin B1 and Cdk1 in the liver after PH was analysed by Western blot. Representative gels (B) and densitometric analyses (C,D) are depicted, n>3.

Based on the *RNA-seq* results, it was demonstrated that Brg1 impairs liver regeneration by modulating the cell cycle pathway. In particular, Cyclin B and Cdk1 showed a significantly positive modulation by Brg1 after PH. Therefore, the protein levels of both Cyclin B and Cdk1 during the liver regeneration phase were analysed by Western blot showing a significantly lower expression of Cyclin B1 and Cdk1 in the Brg1 KO group compared to the Control group 40h and 48h after PH (Fig. 14B-D).

To further investigate the possible mechanisms of cell cycle activation, we performed Gene Set Variation Analysis (GSVA) on each sample at 48 hours post-PH. In contrast to other gene set testing methods, it can account for heterogeneous pathway activity, e.g. pathways are activated by different genes in different samples within an experimental group. It was shown that in particular the p53 pathway is up-regulated in the Brg1 KO group compared to the Control group (Fig 15A). P53 has a key role for cell cycle regulation by different mechanisms. The expression of p53 on protein level was analysed and a significant up-regulation of p53 in Brg1 KO group compared to Control group was demonstrated (Fig. 15B-C). These data confirmed the findings of GSVA of RNA-sequencing. Taken together, these results indicate that in hepatocytes Brg1 influence the cell cycle by modulating cyclins, in particular Cyclin B1 and Cdk1.

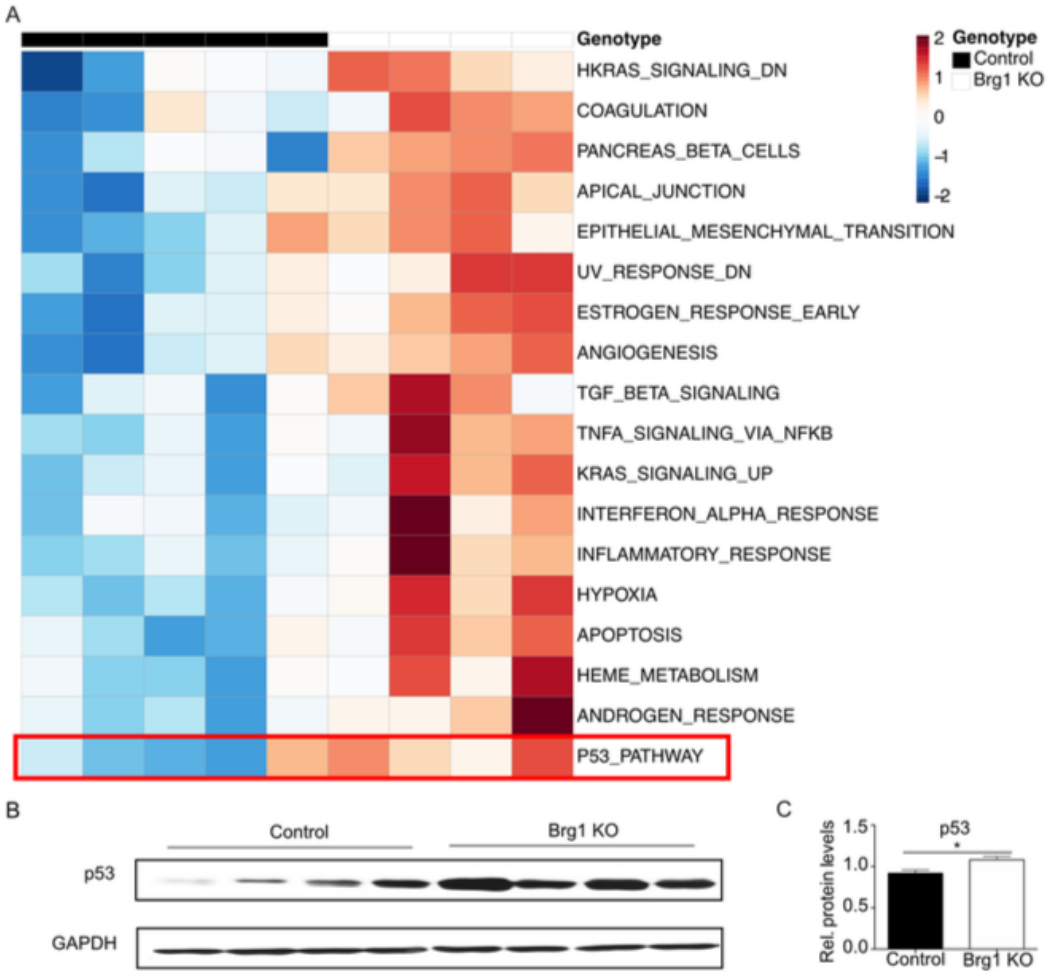

Figure 15. Brg1 regulates cell cycle via p53 pathway

(A) Heatmap of GSVA analysis results at 48h after PH. The z-transformed enrichment scores for significantly associated pathways with the Brg1 genotype are shown. The colour scale represents z-transformed enrichment scores for significantly associated pathways. The green colour corresponds to up-regulated pathways and the blue colour corresponds to the down-regulated pathway. (B,C) Analysis of protein expression of p53 by Western blot in the liver at 48h post PH. Representative gels (B) and densitometric analyses (C) are depicted, n=4.

4.3 Hepatocyte-specific deletion of Brg1 prevents CCl_4-induced liver fibrosis in mice model

4.3.1 Brg1 expression increases after CCl_4 injection

To investigate the role of Brg1 in liver fibrosis, we used the CCl_4-induced liver fibrosis mice model. CCl_4 is the most frequently used hepatotoxin in rodent liver fibrosis and cirrhosis studies. Hepatic Brg1 expression was assessed, before and at different time points after CCl_4 injection in mice to explore the regulation of Brg1 during liver fibrosis.

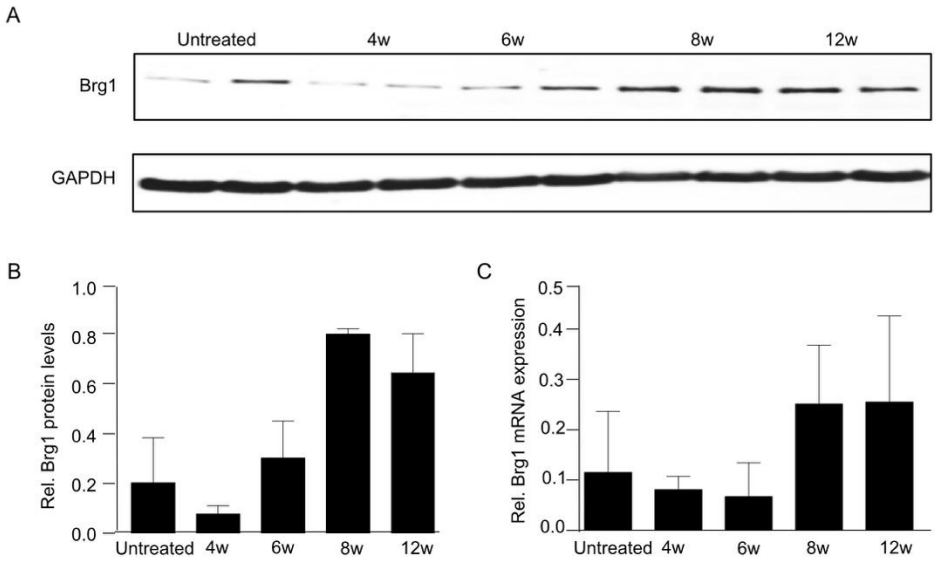

Figure 16. Expression of Brg1 in the liver during fibrogenesis
(A, B) Protein expression of Brg1 in the liver before and after CCl_4 injection were analysed by Western blot. Representative gels (A) and densitometric analyses (B) are depicted, n=4. (C) mRNA expression of Brg1 after CCl_4 injection, n=4.

Weak Brg1 expression was observed in the healthy liver. At the early stage of liver fibrosis (4 weeks and 6 weeks), there was no significant alteration of the Brg1 expression on mRNA or protein levels (Fig. 16 A-C). Both the protein and mRNA levels of Brg1 started to increase gradually when liver fibrosis proceeded. Eight weeks after CCl_4 injection, protein and mRNA levels of Brg1

showed the highest expression (Fig. 16A-C). Brg1 protein expression was increased by approximately 4.0-fold after 8 weeks.

4.3.2 Brg1 knockout decreases CCl_4-induced liver fibrosis

Next, we investigated the effects of Brg1 deletion on CCl_4-induced liver injury and liver fibrosis. The increase in liver body ratio indicates liver injury. Over time (6 weeks and 12 weeks after CCl_4 injection), the liver/body weight ratio of the Brg1 KO group was significantly lower than that of the Control group (Fig.17A). The Alanin-Aminotransferase (Schulze, Stoss et al.) in serum was examined to measure liver injury (Fig. 17B). It was shown that in the serum of the Control group, ALT has a significantly higher indicators level than the Brg1 KO group 6 and 8 weeks after CCl_4 injection.

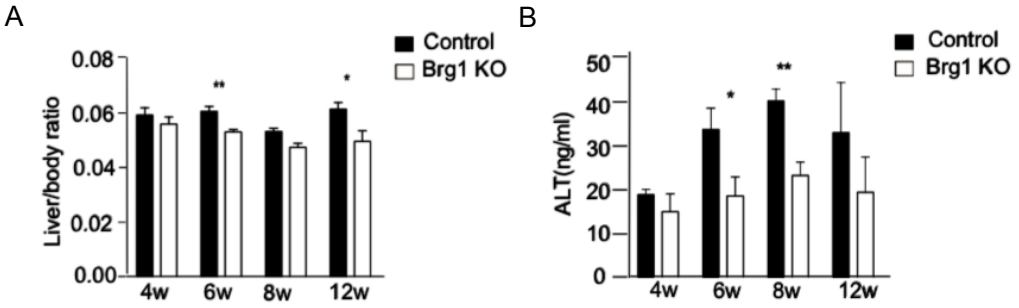

Figure 17. Liver/Body ratio and ALT level of control and Brg1 KO group after CCl_4 injection

(A) Liver to body weight ratios were determined at the indicated time points after CCl_4 injection, n=6. (B) ALT levels were measured using serum samples of Control and Brg1 KO mice after CCl_4 injection, n=3.

Changes in the structure of the mouse hepatic tissues were estimated using H&E staining (Fig. 18A). Hepatic steatosis and lobular structure damage were alleviated in the Brg1 KO group compared to the Control group according to fibrosis score (Fig.18B).

Sirius red staining was used to assess the collagen fibrils in liver tissues of the CCl_4 model mice. In both groups, collagen deposition was obviously observed

in the liver. The density of fibrous deposition in the liver from Brg1 KO group was significantly decreased compared with that of the Control group (Fig.18C-D).

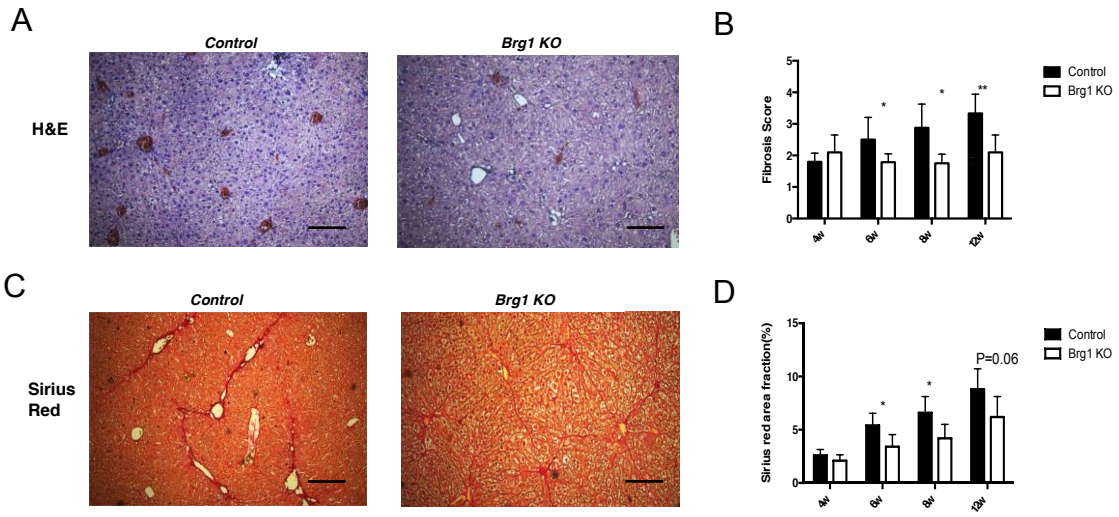

Figure 18. Deletion of Brg1 prevents liver fibrosis after CCl_4 injection in mice
(A) Representative H&E staining of the liver of Control and Brg1 KO group 8 weeks after the start of CCl_4 treatment. (B) Quantification of Fibrosis score at the indicated time points, n=6. (C) Representative Sirius red staining of the liver of Control and Brg1 KO group 8 weeks after CCl_4 injection (bar = 200 μm). (D) Quantification of Sirius red area fraction at the indicated time points, n=6.

Hepatic fibrogenic response is associated with the trans-differentiation of HSCs to myofibroblasts. Alpha smooth muscle-actin (a-SMA) is the maker of CCl_4-induced hepatic stellate cell activation. To investigate the expression of a-SMA in the Brg1 KO group and Control group, we used immunohistochemistry (IHC) and Western blotting to analyse the expression of a-SMA in Control and Brg1 KO mice. The relative expression of the α-SMA protein in Brg1 KO group was significantly lower than that in the Control group at 6 weeks and 8 weeks after CCl_4 injection (Fig.19A, B). The percentage of positive α-SMA area in Brg1 KO group was significantly reduced compared to the Control group at 6 weeks and 8 weeks after CCl_4 injection (Fig.19C, D). Taken together, analysis of a-SMA revealed that Brg1 KO mice have decreased a-SMA expression compared to the Control group. This shows that

Brg1 KO group has fewer hepatic stellate cells activated compared to the Control group.

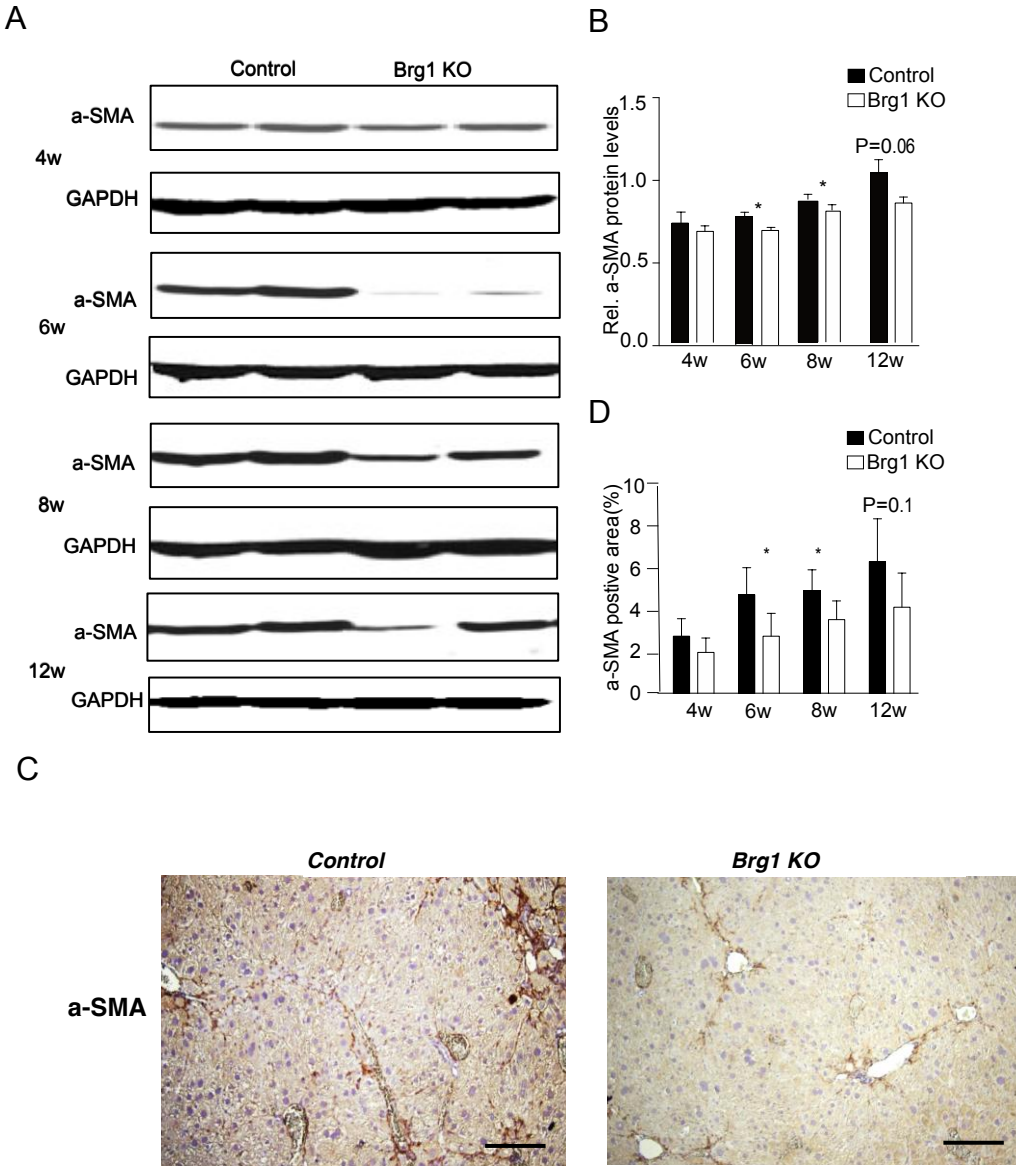

Figure 19. Deletion of Brg1 decreases the expression of α-SMA in the liver after CCl_4 CCl_4 injection in mice

(A) Protein expression of a-SMA in the liver after CCl_4 injection were analysed by Western blot. Representative gels (A) and densitometric analyses (B) are depicted, n=4. (C) Representative immunohistochemical images for a-SMA at 8 weeks after CCl_4 injection in mice(bar = 200 μm). (D) Quantification of a-SMA positive area at the indicated time points, n=6.

4.3.3 Brg1 deletion suppresses TNF-α-NF-κB-mediated inflammatory response in CCl_4-induced fibrosis

Inflammatory mediators, like TNF-α, are involved in CCl_4-induced liver fibrosis (Yang and Seki 2015). Moreover, NF-κB, which promotes inflammatory factors is activated by CCl_4 stimulation (Luedde and Schwabe 2011). We asked whether Brg1 hepatocyte deletion will impact TNF-a/NF-KB pathway in CCl_4 induced liver fibrosis mice model so we used western blot to detect the expression of related proteins.

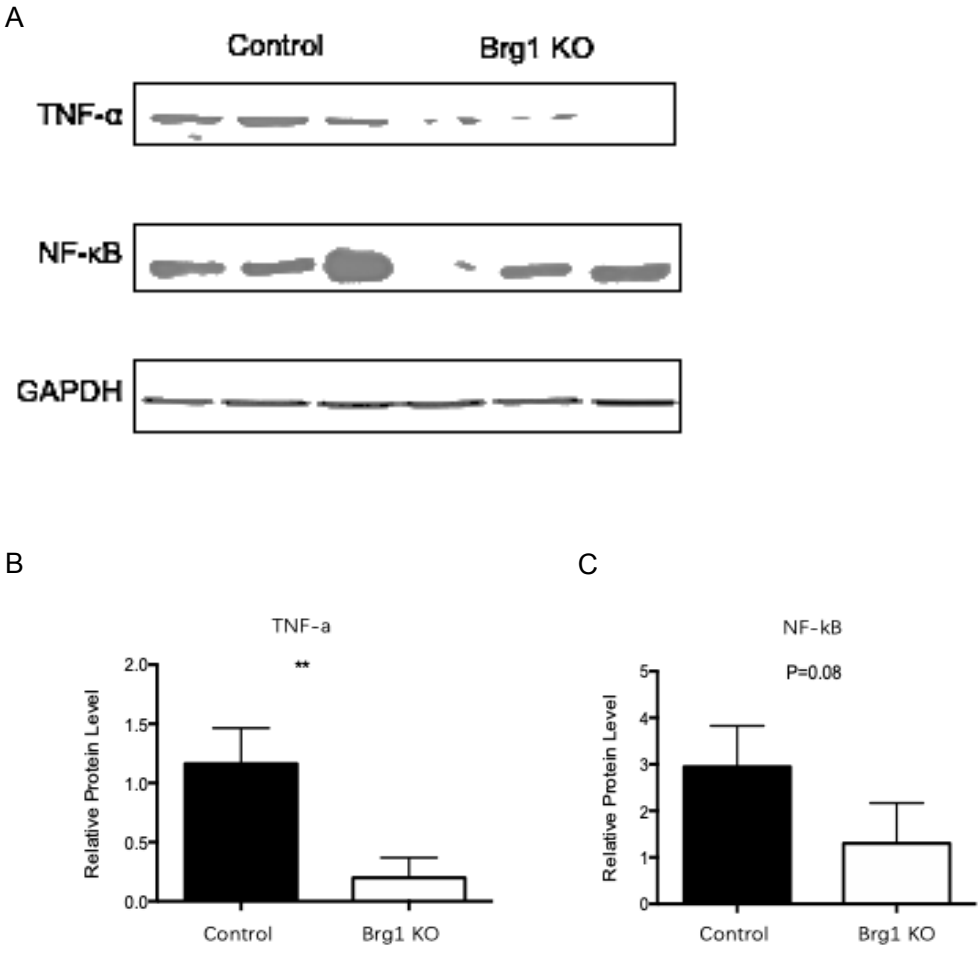

Figure 20. Deletion of Brg1 suppresses TNF-α-NF-κB-mediated inflammatory response in CCl_4-induced fibrosis

Protein expression of TNF-a and NF-κB in the liver after CCl_4 injection was analysed by Western blot. Representative gels are depicted. Representative gels (A) and densitometric analyses (B-C) are depicted, n=3.

It is shown that in Brg1 KO group the expression of TNF-α and NF-κB is lower compared to the Control Group 8 weeks after CCl_4 injection(Fig. 20).

In addition, the expression of genes involved in the recruitment and maintenance of inflammatory cells, including Ccl3, Cxcl2 and Cxcl5 was significantly upregulated in the liver of Control mice compared to Brg1 KO mice 8 weeks after the CCl_4 injection (Fig. 21). These data suggest that Brg1 affects TNF-α-NF-κB-mediated inflammatory response.

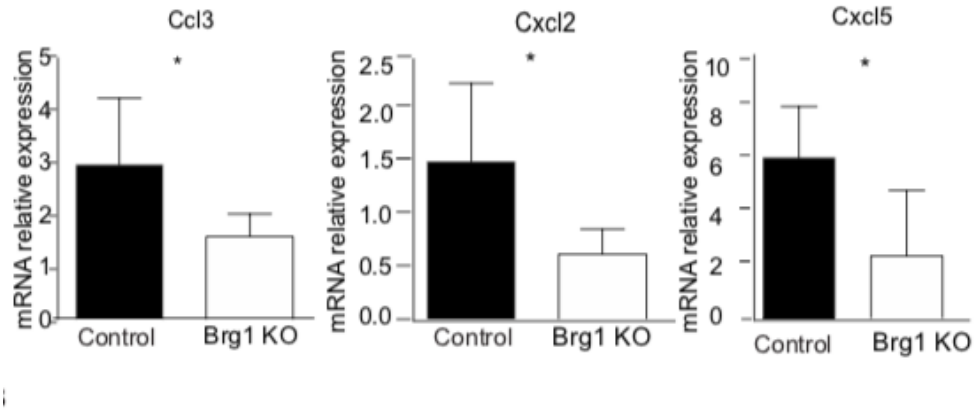

Figure 21. Deletion of Brg1 suppresses inflammatory response in CCl_4-induced fibrosis

mRNA expression of Ccl3, Cxcl2 and Cxcl5 in the liver after CCl_4 injection were analysed by qPCR, n=3.

5 DISCUSSION

5.1 Brg1 positively regulates liver regeneration

Liver regeneration after PH requires the extensive and coordinated proliferation of hepatocytes. Recent studies have indicated that mutations causing Brg1 dysfunction are related to various diseases that are characterised by aberrant cell proliferation (Bultman, Gebuhr et al. 2005, Bultman, Gebuhr et al. 2006). However, the underlying mechanisms by which Brg1 regulates cell proliferation are still not fully understood. In this study, the essential role of Brg1 in liver regeneration was investigated and it was demonstrated that Brg1 is required for the proliferative response of hepatocytes during liver regeneration.

In this study it was shown that Brg1 mRNA and protein levels were transiently up-regulated during liver regeneration and that Brg1 KO mice had a significantly lower proliferation rate and liver-to-body ratio than the Control group 48h after PH. Therefore, these findings underline the important role of Brg1 for tissue regeneration and proliferation in the liver and are in line with previous studies that showed a crucial role of Brg1 for tissue regeneration and proliferation in other organs (Li, Xiong et al. 2013, Xiao, Gao et al. 2016). The data of this study are also in accordance with the expression studies of Sinha et al., which suggested an important role of Brg1 during the injury and regeneration phase of the liver after thioacetamide-induced liver injury. A specific role of Brg1 on proliferation was also shown in HCC by Kaufmann et al. (Kaufmann, Wang et al. 2017).

5.2 Brg1 modulates liver regeneration by regulating the cell cycle pathway

The *RNA-seq* results of this study showed that in the proliferation phase of liver regeneration, the cell cycle pathway is impaired in Brg1 KO mice. Cyclins, especially Cyclin B1, which is induced during the G2 phase of the cell cycle, was decreased in Brg1 KO mice. Consistent with these findings, the expression of the Cdk1 protein that forms a complex with Cyclin B and plays a key role in advancing the cell cycle to the M phase, was also significantly reduced. In line with these data, the regulation of cell cycle genes by Brg1 in order to promote tissue regeneration and proliferation was identified in other organs such as the heart (Xiong, Li et al. 2013, Xiao, Gao et al. 2016). However, an inverse interaction of different cyclin-dependent kinase inhibitors and Brg1 was revealed in these studies as the main way to regulate the cell cycle. These findings indicate that Brg1 regulates the cell cycle in a cell- and context-dependent manner.

The key role of Cyclin B during liver regeneration was recently demonstrated (Sun, Chuang et al. 2016). In contrast to the data of this work, the suppression of the SWI/SNF subunit Arid1a leads to an increase of Cyclin B and promotes liver regeneration (Sun, Chuang et al. 2016). In addition, complete ablation of Arid1a improves the regenerative capacity after liver injury, mainly due to suppression of target genes that inhibit proliferation (Sun, Chuang et al. 2016). This contrary role of individual subunits of the SWI/SNF complex in liver regeneration remains unclear. A possible explanation may be the pattern of genes that each subunit binds. Whereas Brg1 may mainly interact positively with genes promoting liver regeneration, Arid1a may predominantly regulate genes repressing proliferation and regeneration (Sun, Chuang et al. 2016)

In this study, regulation of the p53 pathway by Brg1 in liver regeneration was identified. These findings are in line with previous studies that showed an

inverse correlation between Brg1 and p53 in order to regulate proliferation and cell cycle arrest (He and Luo 2012, Singh, Foley et al. 2016, Wang, Fu et al. 2017). Hereby, Brg1 negatively regulates p53, which is an important gene that modulates cell cycle by different mechanisms on protein level. Interestingly, it is shown that p53 can also bind directly to the Cyclin B1 promoter and therefore inhibit Cyclin B1 transcription (Innocente, Abrahamson et al. 1999). Consequently, during liver regeneration Brg1 KO mice used in this study show an upregulation of p53 protein caused by a lack of Brg1 level. Increased p53 protein expression can lead to a decrease of Cyclin B and subsequently reduced cell proliferation. In addition, not only is the indirect regulation of cyclins by Brg1 via p53 reported. The direct binding of Brg1 to the promoter of Cyclin B was also shown (Raab, Runge et al. 2017). Through this, Brg1 is able to regulate cell cycle by direct regulation of the expression of Cyclin B independent of upstream pathways. Taken together, in our study we were able to show that Brg1 regulates cell cycle by modulating the expression of the cyclin family, presumably in a direct and p53-dependent indirect manner. Interestingly, in a study by Li and colleagues liver proliferation was mainly modulated by Brg1 via the activation of β-catenin activity indicating an additional Brg1-dependent pathway that may impact liver regeneration (Li, Kong et al. 2019).

5.3 The deletion of Brg1 prevents liver fibrosis after CCl_4 injection in mice

Liver fibrosis as a critical illness syndrome has been emphasised as a serious threat to the world's population (Vuppalanchi and Chalasani 2009). Fibrosis may progresses to liver cirrhosis and liver failure, resulting in the major cause of HCC (Zhou, Zhang et al. 2014). Liver fibrosis is driven by inflammatory cell filtration, activation of quiescent hepatic stellate cells (HSCs) and characterised by the accumulation of extracellular matrix（ECM). In recent

years, the molecular mechanisms of fibrogenesis to discover new target agents became more and more important but the mechanisms are not yet fully known. Brg1, as one of the central ATPase catalytic subunits of the SWI/SNF complex, is involved in controlling the chromatin structure, which in turn regulates many physiological and pathological processes (Trotter and Archer 2008). Previous studies have demonstrated that Brg1 expression increases during liver fibrosis but could not reveal the exact role of Brg1 in hepatocytes (Li, Lan et al. 2018). CCl_4 acts continuously on the liver of mice, causing liver cell damage and liver inflammation, activating HSCs and resulting in liver fibrosis (Dong, Chen et al. 2016). Brg1 hepatocyte deficiency mice were used to induce carbon tetrachloride (CCl_4)-induced liver fibrosis and to investigate the molecular mechanisms by which it impacts liver fibrosis. In this study, Brg1 expression was revealed to increase in liver tissue during the progression of fibrosis. The deletion of Brg1 in hepatocytes suppresses the pro-fibrotic response of liver inflammation and attenuates liver fibrosis progression in mice model.

CCl_4-induced liver fibrosis model was used to imitate liver injury. Our data indicate that Brg1 is significantly increased in Control group compared to untreated mice after CCl_4 injection. The liver injury-related indicator ALT in CCl_4-administered Brg1 KO mice is significantly lower compared to Control mice. In addition, the data in this study demonstrate that collagen I expression analysed by H&E and Sirius red staining is significantly decreased in Brg1 KO mice compared to Control mice. These data indicate that Brg1 plays a key role during fibrogenesis after CCl_4-administered liver injury.

The activation of HSCs is considered to be an important marker of hepatic fibrosis, which is characterised by the up-regulation of α-SMA and collagen (Moreira 2007). Our results demonstrate that α-SMA expression is significantly

reduced in Brg1 KO mice compared to control mice after CCl_4 administration, indicating the activation of HSCs via the Brg1 pathway.

Liver tissue injury and liver inflammation are the initiating factors of liver fibrogenesis (Yang and Seki 2015, Koyama and Brenner 2017). Cell damage in liver fibrosis releases chemokines and cytokines that cause inflammatory cell invasion. Thereby, the NF-κB pathway plays a key role as a pro-inflammatory signalling pathway. Activation of the NF-κB pathway is induced by pro-inflammatory cytokines, including TNF-α (Lawrence 2009). Besides the activation of the NF-κB pathway (Schwabe and Brenner 2006), TNF-α can also activate HSCs (Yang and Seki 2015). In order to understand the mechanism by which Brg1 reduces liver damage, cytokine expression was measured in liver tissue. It was shown that the expression of Ccl3, Cxcl2 and Cxcl5 was reduced in Brg1 KO group compared to Control group during fibrogenesis. TNF-α, NF-κB in Brg1 KO mice were reduced in comparison to Control mice. TNF-α/NF-kB has been proven to be down-regulated in Brg1 KO mice, and has a key role in fibrogenesis (Luedde and Schwabe 2011). Our data demonstrate that Brg1 is involved in fibrogenesis and may directly or indirectly promote the development of liver fibrosis by modulating liver inflammation via TNF-a/NF-kB pathway.

5.4 Conclusion

In summary, this study demonstrates the critical role of Brg1 in the regulation of liver regeneration and proliferation by modulating cell cycle genes. In addition, it is shown that Brg1 modulates liver fibrosis by promoting liver inflammation.

The findings of this study highlight the specific role of Brg1 for liver regeneration after liver injury and demonstrate a positive modulation of cyclins and cyclin-dependent kinases by Brg1. However, the exact mechanisms that

regulate the expression of Brg1 and the interaction of Brg1 with target gene sites during liver regeneration are still not fully understood and require further investigation. Therefore, Brg1 represents a novel potential therapeutic target to promote liver proliferation after tissue damage.

This study also shows that HSC activation and inflammation response during CCl_4-induced liver fibrosis are associated with Brg1, which mediates the TNF-a/NF-kB pathway. These results highlight a new aspect of Brg1 in the pathogenesis of liver fibrosis. Thus, Brg1 inhibition appears to be a promising strategy for the prevention of hepatic fibrosis in patients with chronic liver diseases.

5.5 Study limitations and future directions

Brg1 has been demonstrated to play important roles in liver development (Inayoshi, Miyake et al. 2006), but less is known about the role of Brg1 in liver regeneration and liver fibrosis, especially the pathways by which Brg1 modulates liver regeneration and fibrosis.

In our study, it was demonstrated that Brg1 positively regulates the cell cycle by modulating the expression of the cyclin family, presumably in a direct and p53-dependent indirect manner in liver regeneration. In order to understand the direct role of Brg1 in hepatocyte proliferation, primary hepatocyte isolation and *in vitro* experiments have to be analysed by further studies.

Since Brg1 has been found to modulate inflammation and regulate the immune response during liver fibrosis, it is also important to study further target genes of Brg1 during liver injury, which was beyond the scope of our study. The interaction between Brg1 and cytokines during liver fibrosis also needs further investigation for a better understanding of the interaction between hepatocytes and non-parenchymal cells and the involved signaling networks.

Finally, it will be interesting to develop hepatocellular carcinoma (HCC) mice models to study the role of Brg1 in the development of HCC. This will provide a better understanding of the role of Brg1 in different liver diseases.

6 SUMMARY

By using a mouse model with the hepatocyte-specific knockout of Brg1, our study reveals an important function of Brg1 during liver regeneration by promoting hepatocellular proliferation through the modulation of cell cycle genes and liver fibrosis by the regulation of inflammation responses.

In this study, a hepatocyte-specific Brg1 gene knockout mouse model was used to analyse the role of Brg1 in liver regeneration by performing a 70% partial hepatectomy (PH). After PH, Brg1 was significantly up-regulated in wild type mice. Mice with hepatocyte-specific Brg1 gene knockout showed a significantly lower liver-to-body weight ratio 48h post-PH, concomitant with a lower hepatocellular proliferation rate compared to wild type mice. RNA sequencing showed that the expression of several cell cycle genes was dependent on Brg1 in order to regulate liver regeneration. After PH, Brg1 KO showed delayed liver proliferation and cell cycle pathway was found to be down-regulated in the Brg1 KO group.

Brg1 expression was significantly increased in fibrotic liver tissue of wild type mice after CCl_4 injection compared to untreated wild type mice. After CCl_4 treatment, the liver-to-body weight ratio of Brg1 hepatocyte-specific knockout mice was reduced compared to wild type mice and Brg1 knockout mice had lower serum ALT levels compared to wild type mice. Furthermore, less fibrosis and inflammation response was observed in Brg1 knockout mice compared to Control mice. In addition, in the Brg1 KO group, the expression of TNF-α and NF-κB were lower compared to the Control group, indicating that Brg1 modulates fibrosis via the TNF-α/NF-κB pathway.

Taken together, Brg1 regulates liver regeneration via the cell cycle pathway and modulates liver fibrosis via the regulation of inflammation.

7 REFERENCES

Akerberg, B. N., M. L. Sarangam and K. Stankunas (2015). "Endocardial Brg1 disruption illustrates the developmental origins of semilunar valve disease." Dev Biol **407**(1): 158-172.

Bai, J., P. Mei, C. Zhang, F. Chen, C. Li, Z. Pan, H. Liu and J. Zheng (2013). "BRG1 is a prognostic marker and potential therapeutic target in human breast cancer." PLoS One **8**(3): e59772.

Bai, J., P. J. Mei, H. Liu, C. Li, W. Li, Y. P. Wu, Z. Q. Yu and J. N. Zheng (2012). "BRG1 expression is increased in human glioma and controls glioma cell proliferation, migration and invasion in vitro." J Cancer Res Clin Oncol **138**(6): 991-998.

Barker, N., A. Hurlstone, H. Musisi, A. Miles, M. Bienz and H. Clevers (2001). "The chromatin remodelling factor Brg-1 interacts with beta-catenin to promote target gene activation." Embo j **20**(17): 4935-4943.

Basu, S. (2003). "Carbon tetrachloride-induced lipid peroxidation: eicosanoid formation and their regulation by antioxidant nutrients." Toxicology **189**(1-2): 113-127.

Becker, P. B. and J. L. Workman (2013). "Nucleosome remodeling and epigenetics." Cold Spring Harb Perspect Biol **5**(9).

Bissell, D. M. (1990). "Cell-matrix interaction and hepatic fibrosis." Prog Liver Dis **9**: 143-155.

Bochar, D. A., L. Wang, H. Beniya, A. Kinev, Y. Xue, W. S. Lane, W. Wang, F. Kashanchi and R. Shiekhattar (2000). "BRCA1 is associated with a human SWI/SNF-related complex: linking chromatin remodeling to breast cancer."

Cell **102**(2): 257-265.

Bogdanos, D. P., B. Gao and M. E. Gershwin (2013). "Liver immunology." Comprehensive Physiology **3**(2): 567-598.

Boyer, J. L. (2013). "Bile formation and secretion." Comprehensive Physiology **3**(3): 1035-1078.

Braet, F. and E. Wisse (2002). "Structural and functional aspects of liver sinusoidal endothelial cell fenestrae: a review." Comparative hepatology **1**(1): 1-1.

Budhavarapu, V. N., M. Chavez and J. K. Tyler (2013). "How is epigenetic information maintained through DNA replication?" Epigenetics Chromatin **6**(1): 32.

Bultman, S., T. Gebuhr, D. Yee, C. La Mantia, J. Nicholson, A. Gilliam, F. Randazzo, D. Metzger, P. Chambon, G. Crabtree and T. Magnuson (2000). "A Brg1 null mutation in the mouse reveals functional differences among mammalian SWI/SNF complexes." Mol Cell **6**(6): 1287-1295.

Bultman, S. J., T. C. Gebuhr and T. Magnuson (2005). "A Brg1 mutation that uncouples ATPase activity from chromatin remodeling reveals an essential role for SWI/SNF-related complexes in beta-globin expression and erythroid development." Genes Dev **19**(23): 2849-2861.

Bultman, S. J., T. C. Gebuhr, H. Pan, P. Svoboda, R. M. Schultz and T. Magnuson (2006). "Maternal BRG1 regulates zygotic genome activation in the mouse." Genes Dev **20**(13): 1744-1754.

Chi, T. H., M. Wan, P. P. Lee, K. Akashi, D. Metzger, P. Chambon, C. B. Wilson and G. R. Crabtree (2003). "Sequential roles of Brg, the ATPase subunit of BAF chromatin remodeling complexes, in thymocyte development." Immunity

19(2): 169-182.

Cienfuegos, J. A., F. Rotellar, J. Baixauli, F. Martínez-Regueira, F. Pardo and J. L. Hernández-Lizoáin (2014). "Liver regeneration--the best kept secret. A model of tissue injury response." Revista espanola de enfermedades digestivas: organo oficial de la Sociedad Espanola de Patologia Digestiva **106**(3): 171-194.

Clapier, C. R. and B. R. Cairns (2009). "The biology of chromatin remodeling complexes." Annu Rev Biochem **78**: 273-304.

Couinaud, C. (1954). "Anatomic principles of left and right regulated hepatectomy: technics." J Chir (Paris) **70**: 933-966.

de Andrade, K. Q., F. A. Moura, J. M. dos Santos, O. R. de Araújo, J. C. de Farias Santos and M. O. Goulart (2015). "Oxidative Stress and Inflammation in Hepatic Diseases: Therapeutic Possibilities of N-Acetylcysteine." Int J Mol Sci **16**(12): 30269-30308.

Dong, S., Q. L. Chen, Y. N. Song, Y. Sun, B. Wei, X. Y. Li, Y. Y. Hu, P. Liu and S. B. Su (2016). "Mechanisms of CCl4-induced liver fibrosis with combined transcriptomic and proteomic analysis." J Toxicol Sci **41**(4): 561-572.

Eipel, C., K. Abshagen and B. Vollmar (2010). "Regulation of hepatic blood flow: the hepatic arterial buffer response revisited." World journal of gastroenterology **16**(48): 6046-6057.

Eroglu, B., G. Wang, N. Tu, X. Sun and N. F. Mivechi (2006). "Critical role of Brg1 member of the SWI/SNF chromatin remodeling complex during neurogenesis and neural crest induction in zebrafish." Dev Dyn **235**(10): 2722-2735.

Euskirchen, G., R. K. Auerbach and M. Snyder (2012). "SWI/SNF

chromatin-remodeling factors: multiscale analyses and diverse functions." Journal of Biological Chemistry **287**(37): 30897-30905.

Euskirchen, G. M., R. K. Auerbach, E. Davidov, T. A. Gianoulis, G. Zhong, J. Rozowsky, N. Bhardwaj, M. B. Gerstein and M. Snyder (2011). "Diverse roles and interactions of the SWI/SNF chromatin remodeling complex revealed using global approaches." PLoS Genet **7**(3): e1002008.

Fahrner, R., F. Dondorf, M. Ardelt, U. Settmacher and F. Rauchfuss (2016). "Role of NK, NKT cells and macrophages in liver transplantation." World journal of gastroenterology **22**(27): 6135-6144.

Fausto, N. (2004). "Liver regeneration and repair: hepatocytes, progenitor cells, and stem cells." Hepatology **39**(6): 1477-1487.

Fausto, N., J. S. Campbell and K. J. Riehle (2006). "Liver regeneration." Hepatology **43**(S1): S45-S53.

Frevert, U., S. Engelmann, S. Zougbede, J. Stange, B. Ng, K. Matuschewski, L. Liebes and H. Yee (2005). "Intravital observation of Plasmodium berghei sporozoite infection of the liver." PLoS Biol **3**(6): e192.

Fujita, T. and S. Narumiya (2016). "Roles of hepatic stellate cells in liver inflammation: a new perspective." Inflammation and Regeneration **36**(1): 1.

Gambarin-Gelwan, M. (2013). "Viral hepatitis, non-alcoholic fatty liver disease and alcohol as risk factors for hepatocellular carcinoma." Chin Clin Oncol **2**(4): 32.

George, J. and G. Chandrakasan (2000). "Biochemical abnormalities during the progression of hepatic fibrosis induced by dimethylnitrosamine." Clin Biochem **33**(7): 563-570.

Gong, F., D. Fahy and M. J. Smerdon (2006). "Rad4-Rad23 interaction with SWI/SNF links ATP-dependent chromatin remodeling with nucleotide excision repair." Nat Struct Mol Biol **13**(10): 902-907.

Griffin, C. T., J. Brennan and T. Magnuson (2008). "The chromatin-remodeling enzyme BRG1 plays an essential role in primitive erythropoiesis and vascular development." Development **135**(3): 493-500.

Han, P., C. T. Hang, J. Yang and C. P. Chang (2011). "Chromatin remodeling in cardiovascular development and physiology." Circ Res **108**(3): 378-396.

Han, Y. P., L. Zhou, J. Wang, S. Xiong, W. L. Garner, S. W. French and H. Tsukamoto (2004). "Essential role of matrix metalloproteinases in interleukin-1-induced myofibroblastic activation of hepatic stellate cell in collagen." J Biol Chem **279**(6): 4820-4828.

Hang, C. T., J. Yang, P. Han, H. L. Cheng, C. Shang, E. Ashley, B. Zhou and C. P. Chang (2010). "Chromatin regulation by Brg1 underlies heart muscle development and disease." Nature **466**(7302): 62-67.

Hanzelmann, S., R. Castelo and J. Guinney (2013). "GSVA: gene set variation analysis for microarray and RNA-seq data." BMC Bioinformatics **14**: 7.

He, H. and Y. Luo (2012). "Brg1 regulates the transcription of human papillomavirus type 18 E6 and E7 genes." Cell Cycle **11**(3): 617-627.

Heindryckx, F., I. Colle and H. Van Vlierberghe (2009). "Experimental mouse models for hepatocellular carcinoma research." Int J Exp Pathol **90**(4): 367-386.

Hellerbrand, C., B. Stefanovic, F. Giordano, E. R. Burchardt and D. A. Brenner (1999). "The role of TGFbeta1 in initiating hepatic stellate cell activation in vivo." J Hepatol **30**(1): 77-87.

Higgins, G. M. (1931). "Experimental pathology of the liver. I. Restoration of the liver of the white rat following partial surgical removal." Arch pathol **12**: 186-202.

Ho, L. and G. R. Crabtree (2010). "Chromatin remodelling during development." Nature **463**(7280): 474-484.

Hu, J., K. Srivastava, M. Wieland, A. Runge, C. Mogler, E. Besemfelder, D. Terhardt, M. J. Vogel, L. Cao and C. Korn (2014). "Endothelial cell-derived angiopoietin-2 controls liver regeneration as a spatiotemporal rheostat." Science **343**(6169): 416-419.

Hu, N., P. H. Strobl-Mazzulla and M. E. Bronner (2014). "Epigenetic regulation in neural crest development." Dev Biol **396**(2): 159-168.

Inayoshi, Y., K. Miyake, Y. Machida, H. Kaneoka, M. Terajima, T. Dohda, M. Takahashi and S. Iijima (2006). "Mammalian chromatin remodeling complex SWI/SNF is essential for enhanced expression of the albumin gene during liver development." J Biochem **139**(2): 177-188.

Innocente, S. A., J. L. Abrahamson, J. P. Cogswell and J. M. Lee (1999). "p53 regulates a G2 checkpoint through cyclin B1." Proc Natl Acad Sci U S A **96**(5): 2147-2152.

Iwaisako, K., C. Jiang, M. Zhang, M. Cong, T. J. Moore-Morris, T. J. Park, X. Liu, J. Xu, P. Wang, Y. H. Paik, F. Meng, M. Asagiri, L. A. Murray, A. F. Hofmann, T. Iida, C. K. Glass, D. A. Brenner and T. Kisseleva (2014). "Origin of myofibroblasts in the fibrotic liver in mice." Proc Natl Acad Sci U S A **111**(32): E3297-3305.

Josling, G. A., S. A. Selvarajah, M. Petter and M. F. Duffy (2012). "The role of bromodomain proteins in regulating gene expression." Genes (Basel) **3**(2):

320-343.

Kadoch, C. and G. R. Crabtree (2015). "Mammalian SWI/SNF chromatin remodeling complexes and cancer: Mechanistic insights gained from human genomics." Sci Adv **1**(5): e1500447.

Kaufmann, B., B. Wang, S. Zhong, M. Laschinger, P. Patil, M. Lu, V. Assfalg, Z. Cheng, H. Friess, N. Huser, G. von Figura and D. Hartmann (2017). "BRG1 promotes hepatocarcinogenesis by regulating proliferation and invasiveness." PLoS One **12**(7): e0180225.

Kaul, V. and S. J. Munoz (2000). "Coagulopathy of Liver Disease." Current treatment options in gastroenterology **3**(6): 433-438.

Khavari, P. A., C. L. Peterson, J. W. Tamkun, D. B. Mendel and G. R. Crabtree (1993). "BRG1 contains a conserved domain of the SWI2/SNF2 family necessary for normal mitotic growth and transcription." Nature **366**(6451): 170-174.

Kholodenko, I. V. and K. N. Yarygin (2017). "Cellular mechanisms of liver regeneration and cell-based therapies of liver diseases." BioMed research international **2017**.

Kmiec, Z. (2001). "Cooperation of liver cells in health and disease." Adv Anat Embryol Cell Biol **161**: Iii-xiii, 1-151.

Koyama, Y. and D. A. Brenner (2017). "Liver inflammation and fibrosis." J Clin Invest **127**(1): 55-64.

Kuleshov, M. V., M. R. Jones, A. D. Rouillard, N. F. Fernandez, Q. Duan, Z. Wang, S. Koplev, S. L. Jenkins, K. M. Jagodnik, A. Lachmann, M. G. McDermott, C. D. Monteiro, G. W. Gundersen and A. Ma'ayan (2016). "Enrichr: a comprehensive gene set enrichment analysis web server 2016 update."

Nucleic Acids Res **44**(W1): W90-97.

Lawrence, T. (2009). "The nuclear factor NF-kappaB pathway in inflammation." Cold Spring Harb Perspect Biol **1**(6): a001651.

Leibing, T., C. Geraud, I. Augustin, M. Boutros, H. G. Augustin, J. G. Okun, C. D. Langhans, J. Zierow, S. A. Wohlfeil, V. Olsavszky, K. Schledzewski, S. Goerdt and P. S. Koch (2018). "Angiocrine Wnt signaling controls liver growth and metabolic maturation in mice." Hepatology **68**(2): 707-722.

Li, H., J. Lan, C. Han, K. Guo, G. Wang, J. Hu, J. Gong, X. Luo and Z. Cao (2018). "Brg1 promotes liver fibrosis via activation of hepatic stellate cells." Exp Cell Res **364**(2): 191-197.

Li, N., M. Kong, S. Zeng, C. Hao, M. Li, L. Li, Z. Xu, M. Zhu and Y. Xu (2019). "Brahma related gene 1 (Brg1) contributes to liver regeneration by epigenetically activating the Wnt/beta-catenin pathway in mice." Faseb j **33**(1): 327-338.

Li, W., Y. Xiong, C. Shang, K. Y. Twu, C. T. Hang, J. Yang, P. Han, C. Y. Lin, C. J. Lin, F. C. Tsai, K. Stankunas, T. Meyer, D. Bernstein, M. Pan and C. P. Chang (2013). "Brg1 governs distinct pathways to direct multiple aspects of mammalian neural crest cell development." Proc Natl Acad Sci U S A **110**(5): 1738-1743.

Lin, H., R. P. Wong, M. Martinka and G. Li (2010). "BRG1 expression is increased in human cutaneous melanoma." Br J Dermatol **163**(3): 502-510.

Love, M. I., W. Huber and S. Anders (2014). "Moderated estimation of fold change and dispersion for RNA-seq data with DESeq2." Genome Biol **15**(12): 550.

Luedde, T. and R. F. Schwabe (2011). "NF-kappaB in the liver--linking injury,

fibrosis and hepatocellular carcinoma." Nat Rev Gastroenterol Hepatol **8**(2): 108-118.

Malato, Y., L. E. Sander, C. Liedtke, M. Al-Masaoudi, F. Tacke, C. Trautwein and N. Beraza (2008). "Hepatocyte-specific inhibitor-of-kappaB-kinase deletion triggers the innate immune response and promotes earlier cell proliferation during liver regeneration." Hepatology **47**(6): 2036-2050.

Medina, P. P. and M. Sanchez-Cespedes (2008). "Involvement of the chromatin-remodeling factor BRG1/SMARCA4 in human cancer." Epigenetics **3**(2): 64-68.

Michalopoulos, G. K. (2017). "Hepatostat: Liver regeneration and normal liver tissue maintenance." Hepatology **65**(4): 1384-1392.

Michalopoulos, G. K. and M. C. DeFrances (1997). "Liver regeneration." Science **276**(5309): 60-66.

Mitchell, C. and H. Willenbring (2008). "A reproducible and well-tolerated method for 2/3 partial hepatectomy in mice." Nat Protoc **3**(7): 1167-1170.

Mitchell, C. and H. Willenbring (2008). "A reproducible and well-tolerated method for 2/3 partial hepatectomy in mice." Nature Protocols **3**: 1167.

Mitra, V. and J. Metcalf (2009). "Metabolic functions of the liver." Anaesthesia & Intensive Care Medicine **10**(7): 334-335.

Mogler, C., M. Wieland, C. König, J. Hu, A. Runge, C. Korn, E. Besemfelder, K. Breitkopf-Heinlein, D. Komljenovic and S. Dooley (2015). "Hepatic stellate cell-expressed endosialin balances fibrogenesis and hepatocyte proliferation during liver damage." EMBO molecular medicine **7**(3): 332-338.

Mohrmann, L., K. Langenberg, J. Krijgsveld, A. J. Kal, A. J. Heck and C. P.

Verrijzer (2004). "Differential targeting of two distinct SWI/SNF-related Drosophila chromatin-remodeling complexes." Mol Cell Biol **24**(8): 3077-3088.

Moran-Salvador, E. and J. Mann (2017). "Epigenetics and Liver Fibrosis." Cellular and molecular gastroenterology and hepatology **4**(1): 125-134.

Moreira, R. K. (2007). "Hepatic Stellate Cells and Liver Fibrosis." Archives of Pathology & Laboratory Medicine **131**(11): 1728-1734.

Mormone, E., J. George and N. Nieto (2011). "Molecular pathogenesis of hepatic fibrosis and current therapeutic approaches." Chem Biol Interact **193**(3): 225-231.

Muchardt, C. and M. Yaniv (2001). "When the SWI/SNF complex remodels...the cell cycle." Oncogene **20**(24): 3067-3075.

Murphy, D. J., S. Hardy and D. A. Engel (1999). "Human SWI-SNF component BRG1 represses transcription of the c-fos gene." Mol Cell Biol **19**(4): 2724-2733.

Müsch, A. (2014). "The unique polarity phenotype of hepatocytes." Experimental cell research **328**(2): 276-283.

Nadalin, S., M. Bockhorn, M. Malagó, C. Valentin-Gamazo, A. Frilling and C. E. Broelsch (2006). "Living donor liver transplantation." HPB : the official journal of the International Hepato Pancreato Biliary Association **8**(1): 10-21.

Neigeborn, L. and M. Carlson (1984). "Genes affecting the regulation of SUC2 gene expression by glucose repression in Saccharomyces cerevisiae." Genetics **108**(4): 845-858.

Ohkawa, Y., S. Yoshimura, C. Higashi, C. G. Marfella, C. S. Dacwag, T. Tachibana and A. N. Imbalzano (2007). "Myogenin and the SWI/SNF ATPase

Brg1 maintain myogenic gene expression at different stages of skeletal myogenesis." J Biol Chem **282**(9): 6564-6570.

Pahlavan, P. S., R. E. Feldmann Jr, C. Zavos and J. Kountouras (2006). "Prometheus' challenge: molecular, cellular and systemic aspects of liver regeneration." Journal of Surgical Research **134**(2): 238-251.

Pal, S., R. Yun, A. Datta, L. Lacomis, H. Erdjument-Bromage, J. Kumar, P. Tempst and S. Sif (2003). "mSin3A/histone deacetylase 2- and PRMT5-containing Brg1 complex is involved in transcriptional repression of the Myc target gene cad." Mol Cell Biol **23**(21): 7475-7487.

Palmes, D. and H. U. Spiegel (2004). "Animal models of liver regeneration." Biomaterials **25**(9): 1601-1611.

Parekh, S., C. Ziegenhain, B. Vieth, W. Enard and I. Hellmann (2016). "The impact of amplification on differential expression analyses by RNA-seq." Scientific Reports **6**: 25533.

Park, J. H., E. J. Park, H. S. Lee, S. J. Kim, S. K. Hur, A. N. Imbalzano and J. Kwon (2006). "Mammalian SWI/SNF complexes facilitate DNA double-strand break repair by promoting gamma-H2AX induction." Embo j **25**(17): 3986-3997.

Peterson, C. L. and I. Herskowitz (1992). "Characterization of the yeast SWI1, SWI2, and SWI3 genes, which encode a global activator of transcription." Cell **68**(3): 573-583.

Peterson, C. L. and J. W. Tamkun (1995). "The SWI-SNF complex: a chromatin remodeling machine?" Trends in biochemical sciences **20**(4): 143-146.

Petrik, D., S. E. Latchney, I. Masiulis, S. Yun, Z. Zhang, J. I. Wu and A. J. Eisch

(2015). "Chromatin Remodeling Factor Brg1 Supports the Early Maintenance and Late Responsiveness of Nestin-Lineage Adult Neural Stem and Progenitor Cells." Stem Cells **33**(12): 3655-3665.

Phelan, M. L., S. Sif, G. J. Narlikar and R. E. Kingston (1999). "Reconstitution of a core chromatin remodeling complex from SWI/SNF subunits." Mol Cell **3**(2): 247-253.

Postic, C., M. Shiota, K. D. Niswender, T. L. Jetton, Y. Chen, J. M. Moates, K. D. Shelton, J. Lindner, A. D. Cherrington and M. A. Magnuson (1999). "Dual roles for glucokinase in glucose homeostasis as determined by liver and pancreatic beta cell-specific gene knock-outs using Cre recombinase." J Biol Chem **274**(1): 305-315.

Pradere, J. P., J. Kluwe, S. De Minicis, J. J. Jiao, G. Y. Gwak, D. H. Dapito, M. K. Jang, N. D. Guenther, I. Mederacke, R. Friedman, A. C. Dragomir, C. Aloman and R. F. Schwabe (2013). "Hepatic macrophages but not dendritic cells contribute to liver fibrosis by promoting the survival of activated hepatic stellate cells in mice." Hepatology **58**(4): 1461-1473.

Pulice, J. L. and C. Kadoch (2016). "Composition and Function of Mammalian SWI/SNF Chromatin Remodeling Complexes in Human Disease." Cold Spring Harb Symp Quant Biol **81**: 53-60.

Qi, H. P., Y. Wang, Q. H. Zhang, J. Guo, L. Li, Y. G. Cao, S. Z. Li, X. L. Li, M. M. Shi, W. Xu, B. Y. Li and H. L. Sun (2015). "Activation of Peroxisome Proliferator-Activated Receptor γ (PPARγ) Through NF-κB/Brg1 and TGF-ß₁ Pathways Attenuates Cardiac Remodeling in Pressure-Overloaded Rat Hearts." Cellular Physiology and Biochemistry **35**(3): 899-912.

Raab, J. R., J. S. Runge, C. C. Spear and T. Magnuson (2017). "Co-regulation

of transcription by BRG1 and BRM, two mutually exclusive SWI/SNF ATPase subunits." Epigenetics Chromatin **10**(1): 62.

Sakamoto, T., Z. Liu, N. Murase, T. Ezure, S. Yokomuro, V. Poli and A. J. Demetris (1999). "Mitosis and apoptosis in the liver of interleukin-6–deficient mice after partial hepatectomy." Hepatology **29**(2): 403-411.

Savas, S. and G. Skardasi (2018). "The SWI/SNF complex subunit genes: Their functions, variations, and links to risk and survival outcomes in human cancers." Crit Rev Oncol Hematol **123**: 114-131.

Schaffner, F. and H. Poper (1963). "Capillarization of hepatic sinusoids in man." Gastroenterology **44**: 239-242.

Schulze, S., C. Stoss, M. Lu, B. Wang, M. Laschinger, K. Steiger, F. Altmayr, H. Friess, D. Hartmann, B. Holzmann and N. Huser (2018). "Cytosolic nucleic acid sensors of the innate immune system promote liver regeneration after partial hepatectomy." Sci Rep **8**(1): 12271.

Schwabe, R. F. and D. A. Brenner (2006). "Mechanisms of Liver Injury. I. TNF-α-induced liver injury: role of IKK, JNK, and ROS pathways." American Journal of Physiology-Gastrointestinal and Liver Physiology **290**(4): G583-G589.

Shanahan, F., W. Seghezzi, D. Parry, D. Mahony and E. Lees (1999). "Cyclin E associates with BAF155 and BRG1, components of the mammalian SWI-SNF complex, and alters the ability of BRG1 to induce growth arrest." Mol Cell Biol **19**(2): 1460-1469.

Singh, A. P., J. F. Foley, M. Rubino, M. C. Boyle, A. Tandon, R. Shah and T. K. Archer (2016). "Brg1 Enables Rapid Growth of the Early Embryo by Suppressing Genes That Regulate Apoptosis and Cell Growth Arrest." Mol

Cell Biol **36**(15): 1990-2010.

Singhal, N., J. Graumann, G. Wu, M. J. Arauzo-Bravo, D. W. Han, B. Greber, L. Gentile, M. Mann and H. R. Scholer (2010). "Chromatin-Remodeling Components of the BAF Complex Facilitate Reprogramming." Cell **141**(6): 943-955.

Sinha, S., S. Verma and M. M. Chaturvedi (2016). "Differential Expression of SWI/SNF Chromatin Remodeler Subunits Brahma and Brahma-Related Gene During Drug-Induced Liver Injury and Regeneration in Mouse Model." DNA Cell Biol **35**(8): 373-384.

Skandalakis, J. E., L. J. Skandalakis, P. N. Skandalakis and P. Mirilas (2004). "Hepatic surgical anatomy." Surgical Clinics **84**(2): 413-435.

Smith, G. P. (2013). Chapter 19 - Animal Models of Fibrosis in Human Disease. Animal Models for the Study of Human Disease. P. M. Conn. Boston, Academic Press**:** 435-458.

Smith-Roe, S. L., J. Nakamura, D. Holley, P. D. Chastain, 2nd, G. B. Rosson, D. A. Simpson, J. R. Ridpath, D. G. Kaufman, W. K. Kaufmann and S. J. Bultman (2015). "SWI/SNF complexes are required for full activation of the DNA-damage response." Oncotarget **6**(2): 732-745.

Stankunas, K., C. T. Hang, Z. Y. Tsun, H. Chen, N. V. Lee, J. I. Wu, C. Shang, J. H. Bayle, W. Shou, M. L. Iruela-Arispe and C. P. Chang (2008). "Endocardial Brg1 represses ADAMTS1 to maintain the microenvironment for myocardial morphogenesis." Dev Cell **14**(2): 298-311.

Stern, M., R. Jensen and I. Herskowitz (1984). "Five SWI genes are required for expression of the HO gene in yeast." J Mol Biol **178**(4): 853-868.

Sun, G. and K. D. Irvine (2014). Control of growth during regeneration. Current

topics in developmental biology, Elsevier. **108:** 95-120.

Sun, X., J. C. Chuang, M. Kanchwala, L. Wu, C. Celen, L. Li, H. Liang, S. Zhang, T. Maples, L. H. Nguyen, S. C. Wang, R. A. Signer, M. Sorouri, I. Nassour, X. Liu, J. Xu, M. Wu, Y. Zhao, Y. C. Kuo, Z. Wang, C. Xing and H. Zhu (2016). "Suppression of the SWI/SNF Component Arid1a Promotes Mammalian Regeneration." Cell Stem Cell **18**(4): 456-466.

Tanaka, M. and A. Miyajima (2016). "Liver regeneration and fibrosis after inflammation." Inflammation and regeneration **36**: 19-19.

Tang, L., E. Nogales and C. Ciferri (2010). "Structure and function of SWI/SNF chromatin remodeling complexes and mechanistic implications for transcription." Prog Biophys Mol Biol **102**(2-3): 122-128.

Tarrats, N., A. Moles, A. Morales, C. Garcia-Ruiz, J. C. Fernandez-Checa and M. Mari (2011). "Critical role of tumor necrosis factor receptor 1, but not 2, in hepatic stellate cell proliferation, extracellular matrix remodeling, and liver fibrogenesis." Hepatology **54**(1): 319-327.

Taub, R. (2004). "Liver regeneration: from myth to mechanism." Nature reviews Molecular cell biology **5**(10): 836.

Tian, W., H. Xu, F. Fang, Q. Chen, Y. Xu and A. Shen (2013). "Brahma-related gene 1 bridges epigenetic regulation of proinflammatory cytokine production to steatohepatitis in mice." Hepatology **58**(2): 576-588.

Trost, T., J. Haines, A. Dillon, B. Mersman, M. Robbins, P. Thomas and A. Hubert (2018). "Characterizing the role of SWI/SNF-related chromatin remodeling complexes in planarian regeneration and stem cell function." Stem Cell Res **32**: 91-103.

Trotter, K. W. and T. K. Archer (2008). "The BRG1 transcriptional coregulator."

Nucl Recept Signal **6**: e004.

Tyagi, M., N. Imam, K. Verma and A. K. Patel (2016). "Chromatin remodelers: We are the drivers!!" Nucleus **7**(4): 388-404.

Vuppalanchi, R. and N. Chalasani (2009). "Nonalcoholic fatty liver disease and nonalcoholic steatohepatitis: Selected practical issues in their evaluation and management." Hepatology (Baltimore, Md.) **49**(1): 306-317.

Wang, G., Y. Fu, F. Hu, J. Lan, F. Xu, X. Yang, X. Luo, J. Wang and J. Hu (2017). "Loss of BRG1 induces CRC cell senescence by regulating p53/p21 pathway." Cell Death Dis **8**(2): e2607.

Watanabe, T., S. Semba and H. Yokozaki (2011). "Regulation of PTEN expression by the SWI/SNF chromatin-remodelling protein BRG1 in human colorectal carcinoma cells." Br J Cancer **104**(1): 146-154.

Weng, X., L. Yu, P. Liang, L. Li, X. Dai, B. Zhou, X. Wu, H. Xu, M. Fang, Q. Chen and Y. Xu (2015). "A crosstalk between chromatin remodeling and histone H3K4 methyltransferase complexes in endothelial cells regulates angiotensin II-induced cardiac hypertrophy." J Mol Cell Cardiol **82**: 48-58.

Wilson, B. G. and C. W. M. Roberts (2011). "SWI/SNF nucleosome remodellers and cancer." Nature Reviews Cancer **11**: 481.

Wong, M. C. S. and J. Huang (2018). "The growing burden of liver cirrhosis: implications for preventive measures." Hepatology International **12**(3): 201-203.

Workman, J. L. and R. E. Kingston (1998). "Alteration of nucleosome structure as a mechanism of transcriptional regulation." Annu Rev Biochem **67**: 545-579.

Xi, Q., W. He, X. H. Zhang, H. V. Le and J. Massagué (2008). "Genome-wide impact of the BRG1 SWI/SNF chromatin remodeler on the transforming growth factor beta transcriptional program." J Biol Chem **283**(2): 1146-1155.

Xiao, C., L. Gao, Y. Hou, C. Xu, N. Chang, F. Wang, K. Hu, A. He, Y. Luo, J. Wang, J. Peng, F. Tang, X. Zhu and J. W. Xiong (2016). "Chromatin-remodelling factor Brg1 regulates myocardial proliferation and regeneration in zebrafish." Nat Commun **7**: 13787.

Xiong, Y., W. Li, C. Shang, R. M. Chen, P. Han, J. Yang, K. Stankunas, B. Wu, M. Pan, B. Zhou, M. T. Longaker and C. P. Chang (2013). "Brg1 governs a positive feedback circuit in the hair follicle for tissue regeneration and repair." Dev Cell **25**(2): 169-181.

Yang, J., X. Feng, Q. Zhou, W. Cheng, C. Shang, P. Han, C.-H. Lin, H.-S. V. Chen, T. Quertermous and C.-P. Chang (2016). "Pathological Ace2-to-Ace enzyme switch in the stressed heart is transcriptionally controlled by the endothelial Brg1–FoxM1 complex." Proceedings of the National Academy of Sciences **113**(38): E5628-E5635.

Yang, Y. M. and E. Seki (2015). "TNFα in liver fibrosis." Current pathobiology reports **3**(4): 253-261.

Yanguas, S. C., B. Cogliati, J. Willebrords, M. Maes, I. Colle, B. van den Bossche, C. de Oliveira, W. Andraus, V. A. F. Alves, I. Leclercq and M. Vinken (2016). "Experimental models of liver fibrosis." Arch Toxicol **90**(5): 1025-1048.

Zager, R. A. and A. C. Johnson (2009). "Renal ischemia-reperfusion injury upregulates histone-modifying enzyme systems and alters histone expression at proinflammatory/profibrotic genes." Am J Physiol Renal Physiol **296**(5): F1032-1041.

Zhang, C. Y., W. G. Yuan, P. He, J. H. Lei and C. X. Wang (2016). "Liver fibrosis and hepatic stellate cells: Etiology, pathological hallmarks and therapeutic targets." World J Gastroenterol **22**(48): 10512-10522.

Zhang, M., M. Chen, J. R. Kim, J. Zhou, R. E. Jones, J. D. Tune, G. S. Kassab, D. Metzger, S. Ahlfeld, S. J. Conway and B. P. Herring (2011). "SWI/SNF complexes containing Brahma or Brahma-related gene 1 play distinct roles in smooth muscle development." Mol Cell Biol **31**(13): 2618-2631.

Zhou, W. C., Q. B. Zhang and L. Qiao (2014). "Pathogenesis of liver cirrhosis." World J Gastroenterol **20**(23): 7312-7324.

Part of this thesis was published for:

Wang B, Kaufmann B, Engleitner T, Lu M, Mogler C, Olsavszky V, Öllinger R, Zhong S, Geraud C, Cheng Z, Rad RR, Schmid RM, Friess H, Hüser N, Hartmann D, von Figura G. Brg1 promotes liver regeneration after partial hepatectomy via regulation of cell cycle, Sci Rep. 2019 Feb. 20;9(1):2320.

Parts of this thesis were presented at the following scientific conferences:

1. Scientific Oral Presentations

(1) Brg1 positively regulates liver regeneration after partial hepatectomy in mice, 94. Jahrestagung der Vereinigung der Bayerischen Chirurgen e.V., 07/2017, Würzburg, Germany.
(2) Brg1 positively regulates liver regeneration after partial hepatectomy in mice, 25th UEG Week 2017, 10/2017, Barcelona, Spain.
(3) Deletion of Brg1 prevents liver fibrosis after CCl_4 injection in mice, 26th UEG Week 2018, 10/2018, Vienna, Austria.
(4) Hepatocyte-specific Deletion of Brg1 prevents CCl_4-induced liver fibrosis in mice, 96. Jahrestagung der Vereinigung der Bayerischen Chirurgen e.V., 07/2019, Bamberg, Germany.

2. Talking Poster Presentation

Brg1 positively regulates liver regeneration after partial hepatectomy in mice, 13th World Congress of the International Hepato-Pancreato-Biliary Association, 09/2018, Geneva, Switzerland.

3. Poster Presentation

(1) Hepatocyte-specific deletion of Brg1 prevents CCl_4-induced liver fibrosis in mice, 35. Jahrestagung, German Association of the Study of the Liver, 02/2019, Heidelberg, Germany.

(2) Brg1 promotes liver regeneration after partial hepatectomy via regulation of cell cycle, 136. Kongress Deutsche Gesellschaft für Chirurgie, 03/2019, Munich, Germany.